AD_____

Award Number: DAMD17-99-1-9440

TITLE: Cell Surface Regulation of Matrix Metalloproteinases in Breast Cancer Cells

PRINCIPAL INVESTIGATOR: Rafael A. Fridman, Ph.D.

CONTRACTING ORGANIZATION: Wayne State University
Detroit, Michigan 48202

REPORT DATE: August 2000

TYPE OF REPORT: Annual

PREPARED FOR: U.S. Army Medical Research and Materiel Command
Fort Detrick, Maryland 21702-5012

DISTRIBUTION STATEMENT: Approved for Public Release;
Distribution Unlimited

The views, opinions and/or findings contained in this report are those of the author(s) and should not be construed as an official Department of the Army position, policy or decision unless so designated by other documentation.

# REPORT DOCUMENTATION PAGE

*Form Approved*
*OMB No. 074-0188*

| 1. AGENCY USE ONLY (Leave blank) | 2. REPORT DATE August 2000 | 3. REPORT TYPE AND DATES COVERED Annual (1 Jul 99 – 1 Jul 00) |
|---|---|---|

**4. TITLE AND SUBTITLE**
Cell Surface Regulation of Matrix Metalloproteinases in Breast Cancer Cells

**5. FUNDING NUMBERS**
DAMD17-99-1-9440

**6. AUTHOR(S)**
Rafael A. Fridman, Ph.D.

**7. PERFORMING ORGANIZATION NAME(S) AND ADDRESS(ES)**
Wayne State University
Detroit, Michigan 48202

E-Mail: rfridman@med.wayne.edu

**8. PERFORMING ORGANIZATION REPORT NUMBER**

**9. SPONSORING / MONITORING AGENCY NAME(S) AND ADDRESS(ES)**

U.S. Army Medical Research and Materiel Command
Fort Detrick, Maryland 21702-5012

**10. SPONSORING / MONITORING AGENCY REPORT NUMBER**

**11. SUPPLEMENTARY NOTES**

**12a. DISTRIBUTION / AVAILABILITY STATEMENT**
Approved for Public Release; Distribution Unlimited

**12b. DISTRIBUTION CODE**

**13. ABSTRACT** *(Maximum 200 Words)*

Metastasis is the major cause of death in breast cancer patients and is partly caused by the action of proteolytic enzymes that degrade extracellular matrix (ECM). We have focused on the gelatinases, MMP-2 and MMP-9, two ECM-degrading enzymes that are members of the matrix metalloproteinase (MMP) family of proteases. The gelatinases are associated with the surface of breast cancer cells. MMP-2 surface binding plays a role in activation by MT1-MMP, a membrane-bound MMP that is also expressed in breast cancer. MMP-2 activation is mediated by the action of TIMP-2, a metalloproteinase inhibitor. However, the role of TIMP-2 in pro-MMP-2 activation by MT1-MMP is not clear. Although MMP-9 is identified on the cell surface, the mechanism of MMP-9 surface association and regulation remains to be investigated. The research of the Academic Award during the first year has focused on the mechanisms involved in pro-MMP-2 activation and MMP-9 surface association. We report a detailed characterization of the activation of pro-MMP-2 and the interactions of TIMP-2 and MT1-MMP during this process. We also initiated studies on MMP-9 activation on the cell surface and search for MMP-9-binding proteins.

**14. SUBJECT TERMS**
Metalloproteinases, protease inhibitors, breast cancer, metastasis

**15. NUMBER OF PAGES**
31

**16. PRICE CODE**

| 17. SECURITY CLASSIFICATION OF REPORT Unclassified | 18. SECURITY CLASSIFICATION OF THIS PAGE Unclassified | 19. SECURITY CLASSIFICATION OF ABSTRACT Unclassified | 20. LIMITATION OF ABSTRACT Unlimited |
|---|---|---|---|

NSN 7540-01-280-5500

Standard Form 298 (Rev. 2-89)
Prescribed by ANSI Std. Z39-18
298-102

## Table of Contents

## INTRODUCTION

Background. The matrix metalloproteinase (MMP) family of endopeptidases has been shown to play a central role in the promotion of tumor invasion and angiogenesis in breast carcinomas (1, 2) by their ability to mediate the degradation of extracellular matrix (ECM) components as well as non-ECM proteins. A key aspect of proteolytic degradation in cancer cells involves the targeting of enzymes to the cell surface. Studies with various protease systems have shown that surface association of ECM-degrading proteases in cancer cells regulates enzyme activity and interactions with protease inhibitors (3, 4). To achieve their full potential in pericellular proteolysis, the members of the MMP family evolved into secreted and membrane-tethered multidomain enzymes by incorporating distinct domains that facilitate binding to ECM components and surface molecules in the case of soluble MMPs such as the gelatinases (MMP-2 and MMP-9) and unique domains that anchors the enzyme to the cell surface, in the case of the MT-MMPs.

The gelatinases (MMP-2 and MMP-9) represent a subgroup of MMPs that can degrade basement membrane collagen IV and therefore they have been implicated in metastasis in many human tumors including breast cancer (1). As soluble MMPs, the gelatinases developed unique mechanism of surface association. For example, the latent form of pro-MMP-2 binds to a surface complex of MT1-MMP with TIMP-2, which plays a role in activation of pro-MMP-2 (5). Pro-MMP-9 binds to the cell surface via the $\alpha2(IV)$ chain of collagen IV or via the hyaluronic receptor CD44 (3). However, their roles in MMP-9 regulation are not known. Furthermore, other surface-binding proteins may exist.

MT1-MMP is a member of the MT-MMP subfamily of MMPs that is anchored to the cell surface by the presence of a transmembrane domain (6). MT1-MMP is expressed in both breast cancer cells and in the tumor stroma (7). As membrane-tethered MMP, MT1-MMP plays a key role in pericellular proteolysis and is a known activator of pro-MMP-2 on the cell surface. The activation process involves the action of TIMP-2, which binds to active MT1-MMP forming a surface "receptor" for pro-MMP-2. The interactions of TIMP-2 with MT1-MMP and the role they play in pro-MMP-2 activation and MT1-MMP regulation are not well understood.

Purpose. The purpose and scope of the Academic Award proposal is to focus our research efforts in understanding the cell surface regulation of the gelatinases, MMP-2 and MMP-9, and MT1-MMP with the goal to decipher the role of these enzymes in breast cancer progression.

**BODY**

**Note:** Since the results of the following section have been published, we respectfully request the reviewers to refer to the enclosed publications for details in experimental procedures and results.

1. Studies on MT1-MMP and MMP-2 Regulation. (**J. Biol. Chem. 275, 12080-12089, 2000**). During the first year of the grant (1999-2000), we have focused in studying how MT1-MMP promotes the activation of pro-MMP-2 and the role of TIMP-2 in this process. We chose to carry out these studies with purified proteins in a defined cellular system to avoid interference with other endogenous proteases and inhibitors. We used a recombinant vaccinia system to express MT1-MMP alone or in combination with various levels of TIMP-2 in mammalian cells. We found that TIMP-2 regulates the amount of active MT1-MMP (57 kDa) on the cell surface whereas in the absence of TIMP-2 MT1-MMP undergoes autocatalysis to a 44-kDa form, which displays a N-terminus starting at $G^{285}$ and hence lacks the entire catalytic domain. Neither pro-MT1-MMP (N terminus $S^{24}$) nor the 44-kDa form bound TIMP-2. In contrast, active MT1-MMP (N-terminus $Y^{112}$) formed a complex with TIMP-2 suggesting that regulation of MT1-MMP processing is mediated by a complex of TIMP-2 with the active enzyme. Consistently, TIMP-2 enhanced the activation of pro-MMP-2 by MT1-MMP. Thus, under controlled conditions, TIMP-2 may act as a positive regulator of MT1-MMP activity by promoting the availability of active MT1-MMP on the cell surface and consequently, may support pericellular proteolysis.

During this year (99-2000) of the grant, we have also initiated studies to understand the role of MT1-MMP processing in regulation of enzymatic activity, in particular in promoting pro-MMP-2 activation. We hypothesized that inhibition of MT1-MMP autocatalytic turnover by TIMP-2 is an important aspect of the activation process because inhibition of MT1-MMP causes

5

accumulation of active enzyme on the cell surface. We are testing whether synthetic MMP inhibitor will also inhibit MT1-MMP autocatalysis and will contribute to the activation process.
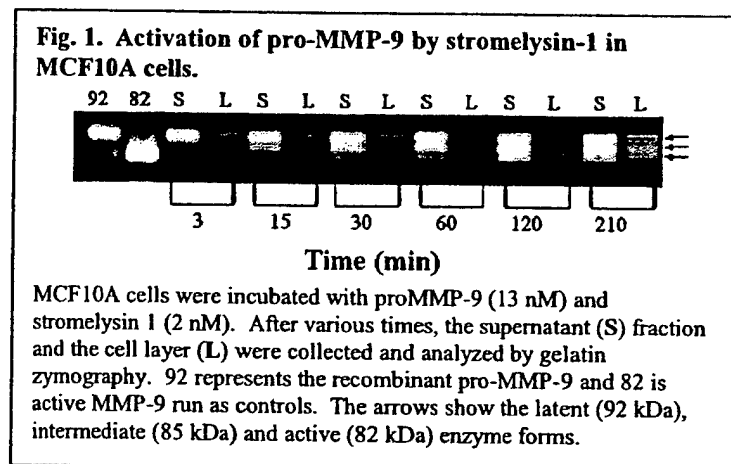
## 2. Studies on MMP-9.

2a. Biochemical Characterization of the Monomeric and Dimeric Forms of MMP-9. (**J. Biol. Chem., 275, 2661-2668, 2000**). During the first year, we completed these studies on MMP-9 characterization. MMP-9 possesses a unique property among members of the MMP family, the ability to exist in a monomeric and a disulfide-bonded dimeric form. We purified to homogeneity the monomeric from the dimeric form of pro-MMP-9 and studied their activation by stromelysin-1, their catalytic competence and their affinities for TIMP-1 and TIMP-2. These studies revealed a significant difference in the rate of activation with the monomer exhibiting a faster rate (one order of magnitude) when compared to the dimer with $K_m$ values in the nanomolar range and relative low $k_{cat}$ values. These studies suggest that, the existence of the slow-activating dimer of pro-MMP-9 may provide an additional level of control during ECM degradation by active MMP-9 species.

2b. Surface Association of MMP-9. MMP-9 has been shown to be associated with tumor metastasis and angiogenesis and is also highly expressed in breast carcinomas (8). We have previously reported that in a series of breast carcinomas samples, MMP-9 protein was partly detected in the surface of the carcinoma cells (9). We then reported that cultured breast epithelial cells exhibit surface-associated MMP-9 (10). Furthermore, we identified the α2(IV) chain of collagen IV as one of the major surface binding proteins for MMP-9 in both immortalized MCF10A breast epithelial cells and MDA-MB-231 breast cancer cells (11). However, the significance of this binding for MMP-9 function remains to be determined.
During the first year of this proposal, we carried out several studies to determine the effect of MMP-9 binding on enzymatic activity. However, these studies are ongoing and have not produced significant and reliable data. Following is a short summary of these studies.

*Activation of pro-MMP-9. Soluble vs. Bound.* To determine the significance of surface association of pro-MMP-9, we studied the rate of pro-MMP-9 activation in breast epithelial

MCF10A cells that were incubated with exogenous pro-MMP-9. Briefly, cells in 24-well plates were incubated (45 min, 4°C) with pro-MMP-9 (various concentrations) to allow enzyme binding and then rinsed to remove unbound zymogen. The cells were then exposed to stromelysin-1 (at a concentration at least 10-fold lower than the amount of added pro-MMP-9). After various times, the serum-free media were collected and analyzed for activity using a fluorescent synthetic peptide substrate MOCAc-Pro-Leu-Gly-LeuA$_2$pr(Dnp)Ala-Arg-NH2, as we have described (12). As control, pro-MMP-9 was incubated with stromelysin-1 in solution at a 1:10 molar ratio (pro-MMP-9: stromelysin-1).
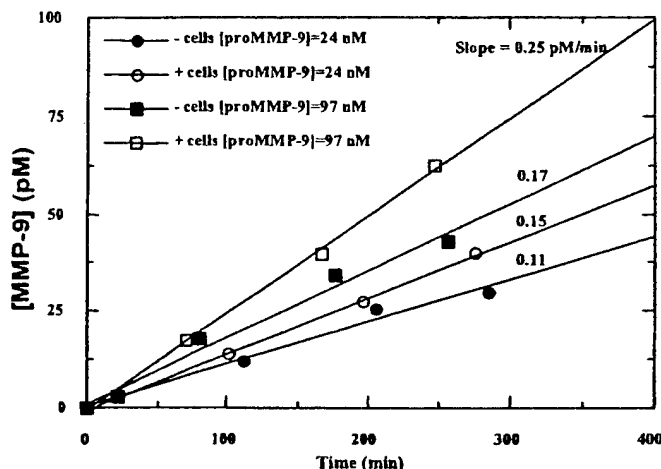
Results: These initial studies failed to provide any meaningful information because of the lack of detection of activity in the media fraction. We believe that the amount of pro-MMP-9 associated with the cells and that is eventually activated by stromelysin-1 is below the detection limit of the assay. To solve the detection problem, in another series of experiments, we decided no to rinse the cells after addition of the exogenous pro-MMP-9 and to collect the supernatant and the cell lysate for analysis by gelatin zymography. As shown in **Fig. 1**, a time-dependent processing of pro-MMP-9 into an 85-kDa intermediate form followed by the formation of the 82-kDa active species was observed.



**Fig. 1. Activation of pro-MMP-9 by stromelysin-1 in MCF10A cells.**

MCF10A cells were incubated with proMMP-9 (13 nM) and stromelysin 1 (2 nM). After various times, the supernatant (S) fraction and the cell layer (L) were collected and analyzed by gelatin zymography. 92 represents the recombinant pro-MMP-9 and 82 is active MMP-9 run as controls. The arrows show the latent (92 kDa), intermediate (85 kDa) and active (82 kDa) enzyme forms.

The 85- and 82-kDa forms could be detected in the cell lysate even after a 3-min incubation whereas none was detected in the media suggesting that the activation reaction proceeded faster on the cell surface. Moreover, a significant fraction of the enzyme remained bound to the cells after a 2-h incubation. We proceeded to follow stromelysin-1 activation of proMMP-9 by monitoring the generation of MMP-9 enzymatic activity with a synthetic fluorogenic peptide substrate as previously described. Two preliminary experiments showed a 1.5-fold enhancement in the initial rate of MMP-9 generation in the presence of cells compared to zymogen activated in solution (**Fig. 2**).

**Fig. 2. Effect of MCF10A cells on the rate of activation of pro-MMP-9 by stromelysin-1**

Various concentrations (24 and 97 nM) of pro-MMP-9 were incubated in the presence or absence of MCF10A cells with 10 nM active stromelysin-1. At various times, the activity of MMP-9 was detected using a fluorigenic peptide substrate.

Although these studies look promising, the interpretation of the data is not straightforward since it is difficult to determine whether the activation process occurred on the cell surface or in solution. We have noticed that upon zymogen binding to the cells, pro-MMP-9 is released from the cell surface and after 10-15 min; a significant amount of enzyme could be detected in the supernatant. This indicates that the enzyme rapidly dissociates from the cells. Given this observation, studies on surface activation will have to determine with certainty that activation indeed occurs at the cell surface and not in the extracellular space. So far, the present results suggest that there is a cell effect on activation but its nature remains undefined.

*Identification of pro-MMP-9 Interacting Proteins.* Since pro-MMP-9 binds to the surface of breast cancer cells, we set up to identify novel proteins that may interact with pro-MMP-9. In our original application we proposed to utilize a biochemical approach using immobilized MMP-9 and cell extracts. Instead, we decided to try a genetic approach using phage display. We thought that this system would allow us to identify interacting proteins and obtain their gene sequence directly. To this end, we initiated studies on affinity screening of a T7 Phage displayed breast tumor cDNA library. The tumor used for making this random primed Human cDNA library (Novagen, WI) was from a 46-year old woman suffering from moderately differentiated invasive ductal carcinoma. The number of primary clones in the library was $1.6 \times 10^7$. The recombinant human pro-MMP-9 used for biopanning was the 92-kDa latent form produced in the lab using our vaccinia expression system in mammalian cells (13). Recombinant pro-MMP-9 was purified to homogeneity as described (12). Trace amounts of TIMP-1 in the recombinant

pro-MMP-9 preparation were removed by Heparin-agarose affinity. During this year (99-00), we set up the conditions for the screening assay as follows:

1.  Each well of ELISA plate was coated with 1µg pro MMP-9. Control wells were coated with BSA alone.

2.  The non-specific binding sites were blocked with 5% protease free BSA

3.  $3.4 \times 10^9$ pfu of the amplified phage display library was added in each well for affinity interaction between phage expressed proteins and pro-MMP9. The plates were incubated for 1h at 37°C to pick up high affinity clones.

4.  The non-binders were washed away with Tris buffered saline containing 0.1% Triton X-100. The stringency of washing increased with each round of screening.

5.  The bound phage was eluted with 0.1%SDS. Eluted phage was amplified on BLT5615 bacterial cells before each round of screening.

At this time, we have screened the library and identified several clones, which will be sequenced. We will report the results of these screening in the next annual report (2000-2001) when we obtain all the information. If this procedure does not produce reliable data, we are also considering the use of the yeast-two hybrid system.

## KEY RESEARCH ACCOMPLISHMENTS

-   Characterized the role of TIMP-2 in pro-MMP-2 activation by MT1-MMP
-   Completed the characterization of the dimeric and monomeric forms of pro-MMP-9
-   Investigated the role of surface binding of pro-MMP-9 in activation of zymogen
-   Initiated search of MMP-9 binding proteins using a phage display system

## REPORTABLE OUTCOMES

<u>Published papers</u>.

1. Olson, M.W., Bernardo, M.M., Pietila, M., Gervasi, D.C., Kotra, L.P., Massova, I., Mobashery, S., and Fridman, R. (2000). Characterization of the monomeric and dimeric forms of latent and active matrix metalloproteinase-9. Differential rates for activation by stromelysin 1. J. Biol. Chem., 275, 2661-2668.

2. Hernandez-Barrantes, S., Toth, M., Bernardo, M.M., Yurkova, M., Gervasi, D.C., Raz, Y., Sang, Q-X. A., and Fridman, R. (2000). Binding of active (57 kDa) membrane type 1-matrix metalloproteinase (MT1-MMP) to tissue inhibitor of metalloproteinase (TIMP)-2 regulates MT1-MMP processing and pro-MMP-2 activation. J. Biol. Chem., 275, 12080-12089.

<u>Abstracts</u>.

1. Bernardo, M.M., Toth, M., Hernandez-Barrantes, S., Gervasi, D., and Fridman, R. "TIMP-2 Regulation Of Pro-MMP-2 Activation By MT1-MMP." International Meeting on Proteinase Inhibitors and Activators. Strategic Targets for Therapeutic Interventions. University of Oxford, England, UK April 17-20, 2000.

Pro-MMP-2 activation has been shown to be mediated by a ternary complex formed by TIMP-2 acting as a molecular link between active MT1-MMP and pro-MMP-2. However, the role of TIMP-2 in the activation process and its effect on MMP-2 activity are still poorly understood. To investigate this process, we developed a mammalian cell-based system to express MT1-MMP in the absence and presence of TIMP-2 using recombinant vaccinia viruses. We measured the net activity, cellular distribution and complex formation with TIMP-2 of active MMP-2 as a function of TIMP-2 expression. MMP-2 activity in the supernatant was dependent on the amount of TIMP-2 expressed with inhibition of activity at high inhibitor concentrations. Interestingly, cleavage of the prodomain of pro-MMP-2 was observed even at the highest inhibitor level. Titration of free TIMP-2 with MMP-2 indicated that the inhibitor in the media

was in complex with MMP-2. Analogous results were obtained with plasma membranes (PMs) of cells co-infected to express MT1-MMP and TIMP-2. Moreover, the PMs inhibited exogenous MMP-2 in a TIMP-2-dependent manner suggesting that MMP-2 can displace membrane-bound TIMP-2. These results suggest that MMP-2 formation results from the interaction of the active MT1-MMP (57 kDa) with pro-MMP-2 as well as with the ternary complex depending on the relative amounts of TIMP-2 and MT1-MMP in the cells. A C-terminal truncated TIMP-2, unable to bind pro-MMP-2, and marimastat, a synthetic MMP inhibitor, induced accumulation of active MT1-MMP and consequently resulted in pro-MMP-2 activation by MT1-MMP demonstrating that ternary complex formation is not an absolute requirement for pro-MMP-2 activation by MT1-MMP.

## CONCLUSIONS

1. We have shown that the surface association of pro-MMP-2 is dependent on the presence of MT1-MMP and TIMP-2. In the absence of TIMP-2 we could not detect cell association and activation of pro-MMP-2 suggesting that the presence of TIMP-2 is necessary for the surface binding of pro-MMP-2 likely to a TIMP-2/MT1-MMP complex. We demonstrated that TIMP-2 can enhance the activation of pro-MMP-2 by MT1-MMp in a cellular system and that this effect is due to ternary complex formation. In addition, the positive effect of TIMP-2 on activation is due to stabilization of MT1-MMP on the cell surface. We characterized the forms of MT1-MMP on the cell surface and the processing of the enzyme in the presence and absence of inhibitor.

2. We completed the characterization of the two major forms of pro-MMP-9, the monomeric and dimeric species, which were also identified in an extract of a breast tumor. These studies demonstrated that both forms bind TIMP-1 and possess similar enzymatic activity. However, the dimeric form is activated at a slower rate by stromelysin-1. We carried out computer modeling of the prodomain of pro-MMP-9 and show that the second cleavage site for stromelysin-1 activation is buried and proposed that the dimeric form must undergoes a change in conformation to expose this site.

3. Preliminary studies on surface activation of pro-MMP-9 have been carried out using MCF10A cells known to bind the enzymes. These studies are undergoing but initial experiments have provided conflicting data due to problems in sensitivity after removing the unbound enzyme. In another series studies, in which pro-MMP-9 was added to the cells but not removed, we observed a 1.5-fold increase in pro-MMP-9 activation by stromelysin-1 in the presence of cells. These studies are unclear since we cannot determine whether this increase in rate of activation is due to surface binding of the zymogen.

4. We have carried out phage display studies to search for pro-MMP-9 binding proteins.

## REFERENCES

1. W. G. Stetler-Stevenson, L. A. Liotta, P. D. Brown, *Cancer Treat Res* **61**, 21-41 (1992).

2. K. J. Heppner, L. M. Matrisian, R. A. Jensen, W. H. Rodgers, *Am J Pathol* **149**, 273-82 (1996).

3. I. Stamenkovic, *Semin Cancer Biol* **10**, 415-33. (2000).

4. P. A. Andreasen, L. Kjoller, L. Christensen, M. J. Duffy, *Int J Cancer* **72**, 1-22 (1997).

5. W. G. Stetler-Stevenson, A. E. Yu, *Semin Cancer Biol* **11**, 143-53. (2001).

6. H. Sato *et al.*, *Nature* **370**, 61-5 (1994).

7. M. Polette *et al.*, *Virchows Arch* **428**, 29-35 (1996).

8. R. Hanemaaijer *et al.*, *Int J Cancer* **86**, 204-7. (2000); M. M. Pacheco, M. Mourao, E. B. Mantovani, I. N. Nishimoto, M. M. Brentani, *Clin Exp Metastasis* **16**, 577-85. (1998).

9. D. W. Visscher *et al.*, *Int J Cancer* **59**, 339-44 (1994).

10. M. Toth, D. C. Gervasi, R. Fridman, *Cancer Res* **57**, 3159-67 (1997).

11. M. W. Olson *et al.*, *J Biol Chem* **273**, 10672-81 (1998); M. Toth, Y. Sado, Y. Ninomiya, R. Fridman, *J Cell Physiol* **180**, 131-9 (1999).

12. M. W. Olson *et al.*, *J Biol Chem* **275**, 2661-8 (2000).

13. R. Fridman *et al.*, *Biochem J* **289**, 411-6 (1993); T. R. Fuerst, P. L. Earl, B. Moss, *Mol Cell Biol* **7**, 2538-44 (1987).

## APPENDICES

1. Olson, M.W., Bernardo, M.M., Pietila, M., Gervasi, D.C., Kotra, L.P., Massova, I., Mobashery, S., and Fridman, R. (2000). Characterization of the monomeric and dimeric forms of latent and active matrix metalloproteinase-9. Differential rates for activation by stromelysin 1. J. Biol. Chem., 275, 2661-2668.

2. Hernandez-Barrantes, S., Toth, M., Bernardo, M.M., Yurkova, M., Gervasi, D.C., Raz, Y., Sang, Q-X. A., and Fridman, R. (2000). Binding of active (57 kDa) membrane type 1-matrix metalloproteinase (MT1-MMP) to tissue inhibitor of metalloproteinase (TIMP)-2 regulates MT1-MMP processing and pro-MMP-2 activation. J. Biol. Chem., 275, 12080-12089.

# Characterization of the Monomeric and Dimeric Forms of Latent and Active Matrix Metalloproteinase-9

## DIFFERENTIAL RATES FOR ACTIVATION BY STROMELYSIN 1*

Matthew W. Olson‡§, M. Margarida Bernardo‡, Martin Pietila‡, David C. Gervasi‡, Marta Toth‡, Lakshmi P. Kotra¶, Irina Massova¶, Shahriar Mobashery¶, and Rafael Fridman‡‖

*From the ‡Department of Pathology and Karmanos Cancer Institute and the ¶Department of Chemistry, Wayne State University, Detroit, Michigan 48201*

Matrix metalloproteinase-9 (MMP-9) is a member of the MMP family that has been associated with degradation of the extracellular matrix in normal and pathological conditions. A unique characteristic of MMP-9 is its ability to exist in a monomeric and a disulfide-bonded dimeric form. However, there exists a paucity of information on the properties of the latent (pro-MMP-9) and active MMP-9 dimer. Here we report the purification to homogeneity of the monomer and dimer forms of pro-MMP-9 and the characterization of their biochemical properties and interactions with tissue inhibitor of metalloproteinase (TIMP)-1 and TIMP-2. Gel filtration and surface plasmon resonance analyses demonstrated that the pro-MMP-9 monomeric and dimeric forms bind TIMP-1 with similar affinities. In contrast, TIMP-2 binds only to the active forms. After activation, the two enzyme forms exhibited equal catalytic competence in the turnover of a synthetic peptide substrate with comparable kinetic parameters for the onset of inhibition with TIMPs and for dissociation of the inhibited complexes. Kinetic analyses of the activation of monomeric and dimeric pro-MMP-9 by stromelysin 1 revealed $K_m$ values in the nanomolar range and relative low $k_{cat}$ values ($1.9 \times 10^{-3}$ and $4.1 \times 10^{-4}$ s$^{-1}$, for the monomer and dimer, respectively) consistent with a faster rate (1 order of magnitude) of activation of the monomeric form by stromelysin 1. This suggests that the rate-limiting event in the activation of pro-MMP-9 may be a requisite slow unfolding of pro-MMP-9 near the site of the hydrolytic cleavage by stromelysin 1.

Matrix metalloproteinase-9 (MMP-9),[1] also known as gelatinase B, is a member of the MMP family of zinc-dependent endopeptidases known for their ability to degrade many extra-

cellular matrix (ECM) components (1, 2). MMP-9 is secreted in a latent form (pro-MMP-9) by a variety of normal and transformed cells and has been implicated in the pathogenesis of several human diseases including arthritis (3), cardiovascular disease (4, 5), and cancer metastasis (6, 7). MMP-9 has also been suggested to play a role in the degradation of ECM during inflammation (8), wound healing (9, 10), trophoblast implantation (11), and angiogenesis (12). Structurally, pro-MMP-9 is closely related to pro-MMP-2 (gelatinase A) with both enzymes containing a fibronectin-like type II module (gelatin-binding domain) inserted into the catalytic domain that is thought to facilitate interaction of the enzymes with collagen molecules (13, 14). The zymogenic forms of both enzymes interact, via their C-terminal domain (hemopexin-like domain), with tissue inhibitors of metalloproteinases (TIMPs), a family of specific endogenous MMP inhibitors (15, 16). Pro-MMP-9 binds to TIMP-1 (1), whereas pro-MMP-2 binds to TIMP-2 (17) and to TIMP-4 (18). After activation, any TIMP molecule efficiently inhibits the enzymatic activity by binding to the catalytic domain of the MMP (16).

Despite the similarities that exist between pro-MMP-9 and pro-MMP-2, the former is unique in several aspects including its gene regulation, structure, and function (2, 14). Pro-MMP-9 is glycosylated and contains an additional 54-amino acid proline-rich insertion of unknown function between the catalytic and the hemopexin-like domains (1). In addition, pro-MMP-9, in contrast to pro-MMP-2, exists in two major forms: a monomeric (~92 kDa) and a disulfide-bonded homodimeric (~220 kDa) form (1). Both the monomeric and dimeric forms of pro-MMP-9 forms have been identified in a variety of pro-MMP-9-producing cells including normal (19–21) and tumor cells (1, 22) and in various biological fluids (23, 24) and tissues (25, 26), indicating that they are physiological forms of the enzyme. In addition, a 125–130-kDa form of pro-MMP-9 present in neutrophil granules has been reported to be a complex of the enzyme with lipocalin (NGAL) (19, 20).

Studies examining the activation, catalytic activity, and interactions with TIMPs of pro-MMP-9 and MMP-9 have focused mainly on the monomeric form of the enzyme. Thus, little is known about the biochemical properties of the homodimeric form. A previous study examined the structural requirements for the formation of the pro-MMP-9 homodimer and its interaction with TIMP-1 (27). However, the kinetics of activation, the catalytic efficiencies, and the inhibition by TIMPs of the monomeric and dimeric forms remained unknown. Here, we report the first comprehensive study aimed at characterizing the biochemical properties of both the latent and active pure monomeric and dimeric forms.

§ Current address: Biochemistry/Molecular Biology, Infectious Disease Research, Wyeth-Ayerst Research, Pearl River, NY 10965.

‖ To whom correspondence should be addressed: Dept. of Pathology, Wayne State University, 540 E. Canfield Ave., Detroit, MI 48201. Tel.: 313-577-1218; Fax: 313-577-8180; E-mail: rfridman@med.wayne.edu.

[1] The abbreviations used are: MMP, matrix metalloproteinase; TIMP, tissue inhibitor of metalloproteinase; ECM, extracellular matrix; PAGE, polyacrylamide gel electrophoresis; SPR, surface plasmon resonance; PBS, phosphate-buffered saline; pro-MMP-9$_M$, pro-MMP-9 monomer; pro-MMP-9$_D$, pro-MMP-9 dimer; mAb, monoclonal antibody; pAb, polyclonal antibody.

14

*Monomeric and Dimeric Forms of Latent and Active MMP-9*

## EXPERIMENTAL PROCEDURES

*Buffers*—Buffer C (50 mM HEPES (pH 7.5), 150 mM NaCl, 5 mM CaCl₂, and 0.02% Brij-35); buffer B (10 mM sodium acetate (pH 4.5)); buffer W (7.8 mM NaH₂PO₄, 8 mM Na₂HPO₄ (pH 7.2), 137 mM NaCl, 0.1 mM CaCl₂, 3 mM KCl, 1.5 mM KH₂PO₄, and 0.02% Tween 20); buffer R (50 mM HEPES (pH 7.5), 150 mM NaCl, 5 mM CaCl₂, 0.01% Brij-35, and 1% (v/v) Me₂SO); buffer D (50 mM Tris (pH 7.4), 150 mM NaCl, 5 mM CaCl₂, and 0.02% Brij-35) and lysis buffer (25 mM Tris-HCl (pH 7.5), 1% Nonidet P-40, 100 mM NaCl, 5 mM EDTA, 20 mM N-ethylmaleimide, 10 μg/ml aprotinin, 1 μg/ml pepstatin A, 1 μg/ml leupeptin, 2 mM benzamidine, and 1 mM phenylmethylsulfonyl fluoride).

*Expression and Purification of Pro-MMP-9 and TIMPs*—Human recombinant pro-MMP-9, TIMP-1, and TIMP-2 were produced in mammalian cells using a recombinant vaccinia virus mammalian cell expression system, as described previously (28). Pro-MMP-9 was purified to homogeneity from the media of infected HeLa cells by gelatin-agarose chromatography, as described previously (29). The concentration of pro-MMP-9 was determined using the molar extinction coefficient of 114,360 M⁻¹ cm⁻¹ (14). Recombinant TIMP-1 and TIMP-2 were purified as described previously (30). Protein concentrations of TIMP-1 and TIMP-2 were determined using their molar extinction coefficients of 26,500 and 39,600 M⁻¹ cm⁻¹, respectively (16).

*Purification of the Monomeric and Dimeric Forms of Pro-MMP-9*—A sample (7600 pmol) of purified pro-MMP-9 diluted in buffer C was layered onto four polyallomer tubes containing a preformed 20–35% glycerol gradient prepared in buffer C. The tubes were then centrifuged (63 h, 4 °C) in a SW41 rotor at 37,000 rpm, after which nine fractions (~200 μl each) were collected and assayed for the presence of monomeric or dimeric forms by gelatin-zymography. Fractions containing homogeneous monomeric (pro-MMP-9ₘ) or dimeric (pro-MMP-9_D) forms were pooled, and their protein concentrations were determined from the molar extinction coefficients: for pro-MMP-9ₘ, 103,645 M⁻¹ cm⁻¹; and for pro-MMP-9_D, 198,609 M⁻¹ cm⁻¹ (31).

*Radioiodination of TIMPs*—TIMP-1 and TIMP-2 were iodinated with carrier free Na¹²⁵I (100 mCi/ml, Amersham Pharmacia Biotech) using IODOGEN (Pierce) as described previously (30). The specific activities of ¹²⁵I-TIMP-1 and ¹²⁵I-TIMP-2 were calculated to be 0.035 and 0.045 μCi/pmol, respectively.

*Size-exclusion Chromatography*—Ten pmol of purified pro-MMP-9ₘ or pro-MMP-9_D were each incubated (1 h, 22 °C) with either ¹²⁵I-TIMP-1 or ¹²⁵I-TIMP-2 (20 pmol with pro-MMP-9ₘ and 30 pmol with pro-MMP-9_D) in a final volume of 0.25 ml. The mixtures were then subjected to gel filtration using a Superose-12 column pre-equilibrated with buffer C. As control, ¹²⁵I-TIMP-1 or ¹²⁵I-TIMP-2 (30 pmol) were chromatographed alone under the same conditions. Fractions (350 μl) were collected and analyzed for radioactivity in a γ counter (Packard model 5650). The amount (picomoles) of ¹²⁵I TIMP-1 or ¹²⁵I-TIMP-2 bound to the pro-MMP-9 forms was determined from the specific activity.

*SDS-PAGE and Gelatin Zymography*—SDS-PAGE was performed according to Laemmli (32). Proteins were visualized by staining overnight with a 0.25% solution of Coomassie Brilliant Blue R-250 in 45% methanol and 10% acetic acid, and destained in a solution of 20% methanol and 10% acetic acid. Gelatin zymography was performed as described (33).

*Preparation of Breast Tumor Extract*—A fresh tissue biopsy (~50 mg) (kindly provided by Dr. D. Visscher, Department of Pathology, Harper Hospital, Detroit, MI) of a breast carcinoma was minced into small pieces and resuspended in 500 μl of cold lysis buffer. The pieces were homogenized on ice with a pestle (Kontes, Vineland, NJ) in a microcentrifuge tube, followed by a centrifugation (14,000 rpm) of the homogenate for 10 min at 4 °C. The supernatant was collected, and the protein concentration was determined by the BCA protein assay (Pierce). The protein concentration was adjusted to 1 μg/μl of 1× sample buffer, and the sample was then subjected to gelatin zymography as described above and to immunoblot analysis, as described (21), using an anti-MMP-9 rabbit polyclonal antibody (pAb 109) raised against a synthetic peptide (APRQRQSTLVLTPGDLRT) from the prodomain of human pro-MMP-9 (a generous gift from Dr. Stetler-Stevenson, NCI, National Institutes of Health, Bethesda, MD).

*Pulse-Chase Analysis of Pro-MMP-9 Biosynthesis*—Monkey kidney BS-C-1 cells (80% confluent) in 60-mm dishes were co-infected with 3 plaque-forming units/cell of vTF7–3 vaccinia virus encoding for T7 RNA polymerase and with 3 plaque-forming units/cell of a recombinant vaccinia virus containing the full-length cDNA of human pro-MMP-9 (vT7-GELB) as described (28). Four hours after infection, the medium was aspirated and the cell monolayer was gently washed with warm PBS.

The cells were incubated (30 min) with 1.5 ml/dish starving medium (Dulbecco's modified Eagle's medium without methionine supplemented with 25 mM Hepes and 0.5% fetal bovine serum). The cells were then pulsed with 500 μCi/ml [³⁵S]methionine in starvation medium (1.5 ml/dish) for 15 min at 37 °C. After the pulse, the dishes were placed on ice, the medium was aspirated and the cells were washed twice with PBS before the addition of 1 ml/dish chase medium (Dulbecco's modified Eagle's medium with 10% fetal bovine serum and 4.8 mM methionine). At the end of the chase periods (0–240 min at 37 °C), the medium was collected; the cells were washed with cold PBS and lysed with 1 ml/dish lysis buffer. The lysates were clarified by a brief centrifugation and were pre-absorbed on protein G-Sepharose beads. The lysates and the media were subjected to immunoprecipitation with either a mAb to pro-MMP-9 (CA-209) or mouse IgG and protein G-Sepharose beads, as described (21). The immunoprecipitates were mixed with Laemmli sample buffer, with or without β-mercaptoethanol, and resolved by 8–16% SDS-PAGE followed by autoradiography.

*Fluorometric Activity Assay for MMP-9ₘ and MMP-9_D*—To obtain the active monomer and dimer, purified pro-MMP-9ₘ (100 pmol) or pro-MMP-9_D (60 pmol) in buffer C were incubated (2 h at 37 °C) with 25 pmol of heat-activated recombinant human stromelysin 1 (MMP-3, a generous gift from Dr. Paul Cannon, Center for Bone and Joint Research, Palo Alto, CA). The activated monomer (MMP-9ₘ) and dimer (MMP-9_D) were then subjected to gelatin-agarose chromatography to remove stromelysin 1, as described (30). Fractions containing MMP-9ₘ or MMP-9_D were detected by gelatin zymography and pooled. Enzyme concentrations were determined by titration with TIMP-1 and from their native molar extinction coefficients of 99,817 and 191,349 M⁻¹ cm⁻¹, respectively, as determined by the method of Gill and von Hippel (31). The activities of the purified MMP-9ₘ and MMP-9_D were assayed using the fluorescence quenched substrate MOCAcPLGLA₂pr(Dnp)-AR-NH₂ (Peptide Institute, Inc. Japan), as described (30, 34). Each assay was carried out at 25 °C in 2 ml (final volume) of buffer R containing enzyme and and/or inhibitor at the indicated concentrations. The substrate concentration was varied from 0.05 to 8.0 μM. The enzyme concentrations were 0.2 and 0.1 nM for MMP-9ₘ and MMP-9_D, respectively. Substrate hydrolysis was monitored using a Photon Technology International (PTI) fluorescence spectrophotometer with excitation and emission wavelengths set at 328 and 393 nm, respectively, controlled by a Pentium™ computer using the RatioMaster™ hardware and FeliX™ software provided by PTI. The excitation and emission band passes were 1 and 3 nm, respectively. Fluorescent measurements were taken with a 4-s integration time. Three initial rate determinations were made for each substrate concentration. The Kₘ and Vₘₐₓ values were determined by non-linear regression analyses using Graph-Pad Prism™ and examined by double-reciprocal analysis by linear regression using LINEST (Microsoft Excel™ version 5.0).

*Degradation of Gelatin by MMP-9ₘ and MMP-9_D*—Increasing concentrations (0.07–0.3 nM) of active site-titrated (with TIMP-1) MMP-9ₘ and MMP-9_D were incubated with 1 μM fluorescein-labeled DQ™ gelatin (Molecular Probes, Eugene, OR) in buffer D, in a total volume of 2 ml. Substrate hydrolysis was monitored over a 1-h period at 25 °C using a PTI spectrofluorometer at excitation and emission wavelengths of 495 and 515 nm, respectively. Excitation and emission band passes were 1 and 3 nm, respectively. Background fluorescence due to DQ™ gelatin was measured with substrate in the absence of enzymes and was subtracted from each trace. A fluorescein (Molecular Probes) standard curve was used to correlate the fluorescence increase with the amount of released fluorescein.

*Kinetic Analysis of the Activation of Pro-MMP-9ₘ and Pro-MMP-9_D by Stromelysin 1*—Human recombinant pro-stromelysin 1 was heat activated at 55 °C for 1 h. The amount of catalytically competent stromelysin 1 was determined by active-site titration with human recombinant TIMP-1. Stromelysin 1 activity was measured with 5 μM fluorogenic peptide substrate MOCAcRPKPVE-Nva-WRK(Dnp)-NH₂ (35) (Peptides International, Louisville, KY) in buffer R, at excitation and emission wavelengths of 325 and 393 nm, respectively. Activation of pro-MMP-9ₘ or pro-MMP-9_D was monitored in reaction mixtures containing 2–120 nM of either substrate and 0.5 nM stromelysin 1 in 70 μl of buffer D at 37 °C. At varying times, aliquots (20 μl) of the reaction mixture were added to acrylic cuvettes containing 2 ml of 7 μM MOCAcPLGLA₂pr(Dnp)-AR-NH₂ in buffer R at 25 °C. Less than 10% of hydrolysis of the fluorogenic substrate was monitored, as described by Knight (36). Hydrolysis of this peptide by stromelysin 1 at the concentrations used (0.5–9 nM) was insignificant when compared with the hydrolysis by MMP-9. The MMP-9 (monomer or dimer) concentrations were calculated using the Michaelis-Menten equation and the kₐₜ and Kₘ values for the reaction of the enzyme (monomer and dimer) with the

fluorogenic substrate, as described above. Initial velocities of pro-MMP-9$_M$ or pro-MMP-9$_D$ activation were determined from the linear increase in MMP-9 concentration as a function of time. The kinetic parameters $k_{cat}$ and $K_m$ were obtained by non-linear least squares fitting of the initial rate dependence on the total pro-MMP-9 concentration to the Michaelis-Menten equation using SCIENTIST (Micro-Math Scientific Software, Salt Lake City, UT). The values for $t_{1/2}$ were calculated from the following general relationship for first-order reactions: $k_{cat} \times t_{1/2} = 0.693$.

*Determination of Kinetic and Equilibrium Constants by SPR*—Interactions of latent and active monomer and dimer pro-MMP-9/MMP-9 with TIMP-1 and TIMP-2 were studied using a Fison Iasys™ instrument. TIMP-1 (69 pmol) and TIMP-2 (42 pmol) were immobilized onto activated CM5 sensor cells (Fison), as described (30). Under these conditions, 320–380 arc s of TIMP-2 and 310–360 arc s of TIMP-1 were covalently coupled. Binding reactions were carried out essentially as described previously (30). The equilibrium constants ($K_d$) were calculated from the rate constants for association ($k_a$) and dissociation ($k_d$) from the equation $K_d = k_d/k_a$. For biphasic binding $K_d = k_{d(2)}/k_{a(1)}$ and $k_{d(1)}/k_{a(2)}$ for the low and high affinity binding sites, respectively. The binding constants for each analyte protein were determined in duplicate using at least six different concentrations of analyte (2–400 nM), in a final volume of 200 µl, where the response increased as a function of analyte concentration. For TIMP-1 and TIMP-2, pro-MMP-9$_M$ and active MMP-9$_M$ were titrated from 10 to 125 nM and proMMP-9$_D$ and active MMP-9$_D$ were titrated from 5 to 75 nM. Furthermore, each analyte protein (100 nM) was subjected to analysis using a derivatized sensor cell to determine the amount of nonspecific binding to the carboxymethyl dextran matrix. No binding of the analyte protein to the underivatized matrix was observed. The binding curves were analyzed using the nonlinear data-fitting program Iasys Fastfit™, using both monophasic and biphasic models to obtain the rate constants. Analysis of the data fit the biphasic model, as we have previously described in detail (30).

*Enzyme Inhibition Studies*—To determine the inhibition constant ($K_i$) of TIMP-1 and TIMP-2 for the active monomer and dimer, the rate constants ($k_{on}$ and $k_{off}$) were determined under the following conditions, and from these the $K_i$ was calculated (i.e. $k_{off}/k_{on}$). The fluorogenic peptide substrate concentration for each assay was 7 µM, a concentration ~5-fold greater than the experimentally determined $K_m$ for the reaction of the substrate with MMP-9$_M$ and MMP-9$_D$. TIMP-1 (0–30 nM) or TIMP-2 (0–60 nM) were added to the fluorogenic substrate solution, and the assay was initiated by addition of enzyme to give a final concentration of 1 nM for MMP-9$_M$ and 0.5 nM for MMP-9$_D$. The reaction was allowed to proceed for 6 min, and the rate of substrate cleavage was measured in triplicate for each inhibitor concentration examined. The first-order rate constant, $k$, was determined from the intersection point of the tangent to the curve at $I = x$ to the curve at $I = 0$ where $k = 1/t$, as described (37), where the data points gave equal increments of product formation as a function of time in the absence of inhibitor. The first-order rate constant, $k$, for each TIMP concentration was plotted as a function of TIMP concentration. The slope and error of the slope of this line gives the on-rate, $k_{on}$, as determined by linear regression using LINEST (Microsoft Excel™ version 5.0). The dissociation rate constants ($k_{off}$) were determined in triplicate as follows. MMP-9$_M$ or MMP-9$_D$ (300 nM) and inhibitors (330 nM) were incubated for 1 h at 25 °C. These reaction mixtures were added to a cuvette containing 2 ml of a 12 µM peptide substrate solution. The final enzyme concentration was 0.5 nM. The recovery of enzyme activity was followed for up to 40 min, and the data were analyzed as described (38). The error of the slope of this line was determined by linear regression using LINEST (Microsoft Excel™ version 5.0). The inhibition constants ($K_i$) were calculated from $K_i = k_{off}/k_{on}$.

*Computer Modeling*—The primary sequence of pro-MMP-9 was obtained from the Swiss-Prot data bank (code COG9_HUMAN, total 707 amino acids). A complete model of pro-MMP-9 was constructed as described below. The signal peptide was removed from the complete sequence, and the remaining sequence was divided into prodomain, catalytic, gelatin-binding, and hemopexin-like domains. Homology models were constructed using the COMPOSER module in Sybyl version 6.4; the modeling of the three-dimensional structure of the catalytic domain of MMP-9 has been published previously (13). The hemopexin-like domain of pro-MMP-9 was modeled using the structures of the hemopexin-like domains of pro-MMP-2 (Protein Data Bank codes 1gen and 1rtg), fibroblast collagenase (code 1fbl), and collagenase-3 (code 1pex), following similar procedures that were used for the modeling of the catalytic domain (13, 39–41). The gelatin-binding domain was modeled using the NMR structure of the fibronectin type-II model
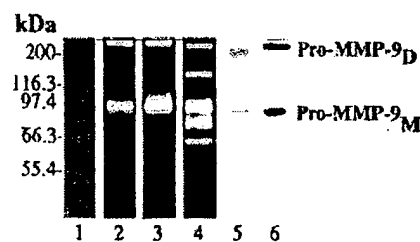


FIG. 1. **Expression of pro-MMP-9$_M$ from pro-MMP-9$_D$.** Samples of recombinant pro-MMP-9 (*lanes 2* and *6*, 10 ng/lane), serum-free conditioned media of tumor necrosis factor-α-treated MCF10A cells (*lane 3*, 20 µl) and of a homogenate of a breast carcinoma biopsy (*lanes 4* and *5*, 30 µg/lane) were subjected to gelatin zymography (*lanes 2–4*) and immunoblot analysis (*lanes 4* and *5*) using a polyclonal antibody (pAb 109) to pro-MMP-9 recognizing the latent form. *Lane 1* shows the molecular weight standards under non reducing conditions.

(code 1fn2) (42). The prodomain of pro-MMP-9 was modeled based on the x-ray structure of homologous prodomain of stromelysin-1 (code 1slm) (43). In modeling the prodomain, residues upstream of 44 were considered in the homology model building because no homologous sequences were found from residues 21–43. Individual domains of human pro-MMP-9 were thus constructed using homology modeling and three-dimensional structure alignment, and the two contiguous domains were organized and linked appropriately in space. The collagen V-like hinge region of pro-MMP-9 was not modeled due to the lack of any homologous protein that could serve as a three-dimensional template. The complete structure of pro-MMP-9 was energy-minimized using AMBER 5.0 software package on a Silicon Graphics Octane workstation with dual processors, for 20,000 cycles (13). However, we have disclosed in this report only the arrangements of the contiguous regions of the prodomain and catalytic domains, since they are pertinent to the discussion. The graphical analysis of the resulting structure was performed using Sybyl software version 6.4.

## RESULTS

*Expression of Pro-MMP-9$_M$ and Pro-MMP-9$_D$*—As shown in the zymogram of Fig. 1, pro-MMP-9 in monomeric (~92 kDa) and dimeric (~210 kDa) forms can be found in preparations of purified recombinant enzyme (Fig. 1, *lane 2*), in serum-free conditioned media of tumor necrosis factor-α-treated non-malignant MCF10A breast epithelial cells (Fig. 1, *lane 3*) and in a tissue homogenate derived from a human breast carcinoma biopsy (Fig. 1, *lane 4*). The tumor sample contains several gelatinolytic bands migrating at ~72, 85, 92, 130, and 225 kDa. To confirm the nature of the MMP-9 forms detected in the tumor homogenate, we carried out an immunoblot analysis using a polyclonal antibody to the prodomain of pro-MMP-9. The tumor homogenate contained two immunoreactive forms of ~92 and 225 kDa (Fig. 1, *lane 5*) consistent with these forms being the monomeric and dimeric forms of pro-MMP-9.

*Biosynthesis of Pro-MMP-9$_M$ and Pro-MMP-9$_D$*—The biosynthesis of pro-MMP-9$_M$ and pro-MMP-9$_D$ was examined by pulse-chase analysis in BSC-1 cells infected with a recombinant vaccinia virus expressing human pro-MMP-9. After the chase period, the resulting media and cell lysates were immunoprecipitated with a mAb against pro-MMP-9 and subjected to SDS-PAGE analysis under non-reducing and reducing conditions followed by autoradiography. As shown in Fig. 2, the pro-MMP-9$_M$ precursor form (~85 kDa) was rapidly synthesized and gradually converted to the fully glycosylated mature form (~92 kDa), which was then secreted into the extracellular space (Fig. 2, *extracellular*). Precursor pro-MMP-9$_D$ (~190 kDa) was clearly noticeable in the lysates as early as 5 min after the pulse, consistent with the dimer being composed of two precursor monomers. Thus, under these conditions, dimerization occurs intracellularly and appears to be independent of glycosylation. After 30 min, a dimer of ~210 kDa was detected in the lysates, possibly representing dimerization of mature monomer forms or, alternatively, complete glycosylation of the
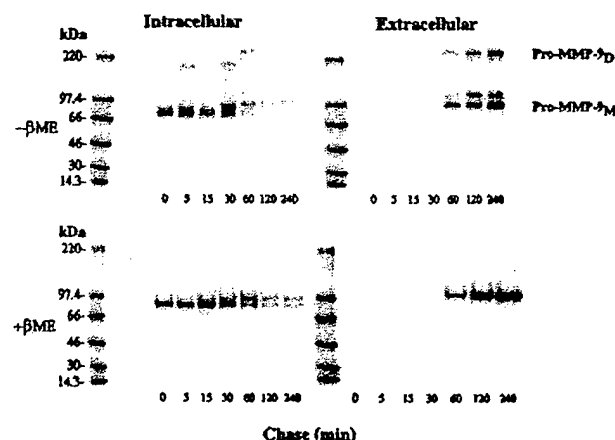
*Monomeric and Dimeric Forms of Latent and Active MMP-9*



FIG. 2. **Pulse-chase analysis of pro-MMP-9 biosynthesis.** Infected BSC-1 cells were subjected to pulse-chase analysis, as described under "Experimental Procedures." At the end of the chase periods (0–240 min), the cells (intracellular) and the media (extracellular) were subjected to immunoprecipitation with an anti-MMP-9 mAb (CA-209). The immunoprecipitates were subjected to 8–16% SDS-PAGE analysis under non-reducing ($-\beta$-ME) or reducing ($+\beta$-ME) conditions followed by autoradiography. $^{14}$C-Labeled molecular weight standards, electrophoresed under reducing conditions, were used as reference.

immature dimer (Fig. 2). After 60 min into the chase period, the mature pro-MMP-9 monomer and dimer were detected in the media (Fig. 2, *extracellular*). In the presence of a reducing agent (Fig. 2, $+\beta$-*mercaptoethanol*), only pro-MMP-9$_M$ was detected (21) consistent with dimerization involving the formation of a disulfide bond (27). Pulse-chase samples prepared in the presence or absence of 20 nM *N*-ethylmaleimide showed similar results demonstrating that dimerization was not a consequence of *in vitro* oxidation during cell lysis (data not shown).

A ~120-kDa protein of unknown origin was also immunoprecipitated from the media and was only observed under non-reducing conditions (Fig. 2, *extracellular*). The 120-kDa protein is not likely to be a complex of the monomeric form with TIMP-1 (31 kDa), as reported by Moll *et al.* (22), since it did not co-immunoprecipitate with a polyclonal antibody to TIMP-1 (data not shown), known to co-precipitate the enzyme/inhibitor complex (21). Consistently, a radiolabeled 31-kDa protein was not detected under reducing conditions in the pulse-chase experiment. Indeed, vaccinia-infected cells do not express endogenous TIMPs (28). Furthermore, a 25-kDa protein, consistent with the molecular mass of lipocalin (19, 20), which is known to form a complex with neutrophil pro-MMP-9, could not be detected under reducing conditions (Fig. 2, $+\beta$-*mercaptoethanol*). Interestingly, the 120-kDa protein was not detected in purified preparations of recombinant pro-MMP-9 (Fig. 3), suggesting that it is a minor component.

*Purification of Pro-MMP-9$_M$ and Pro-MMP-9$_D$*—To characterize the biochemical properties of the pure monomeric and dimeric forms, these forms were isolated from each other using glycerol-gradient sedimentation. Since pro-MMP-9$_D$ sediments faster than pro-MMP-9$_M$, near base-line separations were achieved as shown in the zymogram of Fig. 3A. Gradient fractions containing pro-MMP-9$_M$ or pro-MMP-9$_D$ were pooled, activated or not with stromelysin 1, and examined by non-reducing SDS-PAGE followed by Coomassie Blue staining (Fig. 3B) and by gelatin zymography (Fig. 3C). These analyses revealed that the purified pro-MMP-9$_M$ (Fig. 3, *B* and *C, lane 3*) or pro-MMP-9$_D$ (Fig. 3B, *lane 5*, and *C, lane 4*) were homogeneous. Incubation of pro-MMP-9$_M$ and pro-MMP-9$_D$ with stromelysin 1 resulted in the processing of these two forms to low molecular mass species of ~82 kDa (Fig. 3B, *lane 4*, and *B, lane 5*) and ~200 kDa (Fig. 3, *B* and *C, lane 6*).
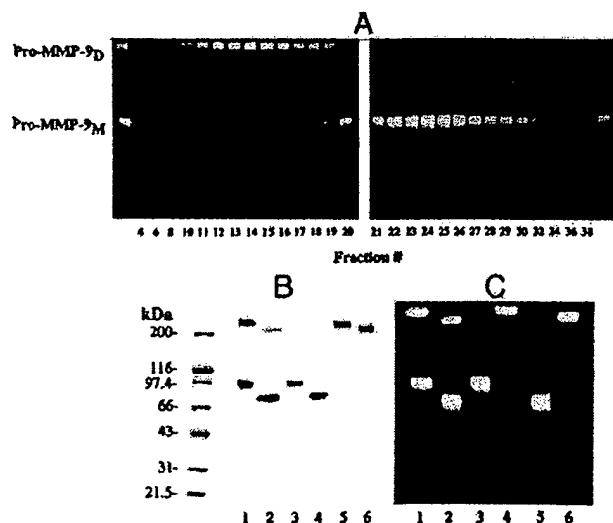


FIG. 3. **Purification of pro-MMP-9$_M$ from pro-MMP-9$_D$ by glycerol-gradient sedimentation.** Recombinant pro-MMP-9 was subjected to glycerol-gradient sedimentation, as described under "Experimental Procedures." *A*, the gradient fractions (1 $\mu$l) were analyzed by gelatin-zymography. *B* and *C*, purified pro-MMP-9$_M$ and pro-MMP-9$_D$ forms were incubated (2 h, 37 °C) with (2B, 2C, 4B, 5C, 6B, and 6C) or without (1B, 1C, 3B, 3C, 4C, and 5B) stromelysin 1. The latent and active forms were analyzed by 8–16% by SDS-PAGE and Coomassie Blue staining under non-reducing conditions (*B*) or by gelatin-zymography (*C*). *Lane 1*, pro-MMP-9; *lane 2*, MMP-9; *lane 3*, purified pro-MMP-9$_M$; *lanes 4B* and *5C* purified MMP-9$_M$; *lanes 5B* and *4C* purified pro-MMP-9$_D$; *lane 6*, purified MMP-9$_D$.

*Catalytic Competence of MMP-9$_M$ and MMP-9$_D$*—We determined the $K_m$ and $k_{cat}$ values for the hydrolysis of the fluorogenic peptide substrate MOCAcPLGLA$_2$pr(Dnp)-AR-NH$_2$ by MMP-9$_M$ and MMP-9$_D$. The data showed saturation kinetics by the two purified enzyme forms similar to that reported for MMP-9, a mixture of monomeric and dimeric forms (30). Nonlinear least-squares fits of the data to the Michaelis-Menten equation allowed for determination of the $K_m$, $k_{cat}$, and $k_{cat}/K_m$ values. The enzymes showed essentially the same affinity for the substrate with $K_m$ values of 1.28 ± 0.08 and 1.32 ± 0.06 $\mu$M for the monomeric and dimeric species, respectively. The $k_{cat}$ and $k_{cat}/K_m$ values for the hydrolysis of the peptide substrate by MMP-9$_M$ and MMP-9$_D$ were also essentially similar with $k_{cat}$ values of 2.72 ± 0.13 and 8.67 ± 0.24 s$^{-1}$ and $k_{cat}/K_m$ values of (2.13 ± 0.14) × 10$^6$ and (6.56 ± 0.22) × 10$^6$ M$^{-1}$ s$^{-1}$, for the monomer and dimer, respectively.

The ability of MMP-9$_M$ and MMP-9$_D$ to degrade a natural substrate was examined using fluorescein-labeled gelatin. These data showed that MMP-9$_M$ and MMP-9$_D$ cleaved the gelatin substrate with similar catalytic efficiency, as indicated by the identical linear dependence of the initial rates of gelatin cleavage as a function of enzyme concentration (0–0.3 nM) (data not shown). Determination of the kinetic parameters ($k_{cat}$ and $K_m$) of this reaction was not possible due to the collisional quenching of the fluorescein-labeled fragments released at the concentrations of gelatin used (25 nM to 1 $\mu$M).

*Differential Kinetics of Activation of Pro-MMP-9$_M$ and Pro-MMP-9$_D$ by Stromelysin 1*—Stromelysin 1 is an efficient activator of pro-MMP-9 (44, 45). Therefore, we wished to compare the kinetics of activation of isolated pro-MMP-9$_M$ and pro-MMP-9$_D$ by stromelysin 1. After exposure of pro-MMP-9$_M$ or pro-MMP-9$_D$ to stromelysin 1, the enzymatic activities of the generated active species were measured using the fluorogenic peptide substrate. Nonlinear least-squares analysis of the data according to the Michaelis-Menten equation provided the kinetic parameters listed in Table I. Thus, pro-MMP-9$_D$ is acti-

TABLE I

*Kinetic parameters for pro-MMP-9 monomer and dimer activation by stromelysin-1*

Increasing concentrations of pro-MMP-9$_M$ and pro-MMP-9$_D$ (2–120 nM) were incubated with 0.5 nM stromelysin 1 in a total volume of 70 μl of buffer D, at 37 °C. MMP-9$_M$ and MMP-9$_D$ were assayed with the fluorogenic substrate (7 μM) in buffer R at 25 °C. Analogous results were obtained from three independent experiments. The kinetic parameters were evaluated from nonlinear regression analysis, as described under "Experimental Procedures."

| Substrate | $K_m$ | $k_{cat}$ | $k_{cat}/K_m$ |
|---|---|---|---|
| | *nM* | $s^{-1}$ | $M^{-1} s^{-1}$ |
| Pro-MMP-9$_M$ | 13 ± 3 | (1.9 ± 0.1) × 10$^{-3}$ | (1.5 ± 0.4) × 10$^5$ |
| Pro-MMP-9$_D$ | 25 ± 7 | (4.1 ± 0.4) × 10$^{-4}$ | (1.6 ± 0.4) × 10$^4$ |

vated with a catalytic efficiency 10-fold lower than that of pro-MMP-9$_M$ due to a difference in the values of $k_{cat}$ since the $K_m$ values are within the experimental error. At subsaturating substrate concentrations, the initial rates of activation of pro-MMP-9$_M$ and pro-MMP-9$_D$ varied linearly with stromelysin 1 concentration and the slopes of the lines correlated with the determined kinetic parameters.

*Pro-MMP-9$_M$ and Pro-MMP-9$_D$ Bind TIMP-1*—Previous experiments in our laboratory, in which pro-MMP-9 and TIMP-1 were co-expressed in the vaccinia expression system, demonstrated that both the monomeric and dimeric forms of the enzyme co-precipitated with TIMP-1 using either anti-TIMP-1 or anti-MMP-9 antibodies.[2] These studies suggested that both pro-MMP-9 forms bind the inhibitor. Here we investigated the ability of purified pro-MMP-9$_M$ and pro-MMP-9$_D$ to form a stable complex with TIMP-1 using size-exclusion chromatography. Prior to gel filtration, purified pro-MMP-9$_M$ or pro-MMP-9$_D$ was incubated with molar excess concentrations of $^{125}$I-TIMP-1 and the mixtures were then chromatographed on a Superose-12 column. Fig. 4 shows the column profiles of $^{125}$I-TIMP-1 alone and of mixtures of $^{125}$I-TIMP-1 with either pro-MMP-9$_M$ or pro-MMP-9$_D$. These column profiles (Fig. 4) and analysis of the eluted fractions by immunoblot and autoradiography (data not shown) demonstrated that a fraction of the $^{125}$I-TIMP-1 co-chromatographed with the monomeric and dimeric forms of proMMP-9 consistent with formation of stable complexes. The sum of the radioactivity present in peak 1 (enzyme/inhibitor complex) and in peak 2 ($^{125}$I-TIMP-1 alone) of the column profiles revealed an enzyme: inhibitor ratio of 1:1.26 for the pro-MMP-9$_M$/TIMP-1 complex and of 1:1.84 for the pro-MMP-9$_D$/TIMP-1 complex consistent with a stoichiometry of 1:1 and 1:2, respectively. As controls, mixtures of either pro-MMP-9$_M$ or pro-MMP-9$_D$ with $^{125}$I-TIMP-2 chromatographed under the same conditions failed to demonstrate complex formation (data not shown). These experiments demonstrate that both the monomeric and dimeric forms of pro-MMP-9 bind TIMP-1.

*SPR Analyses of Latent and Active Monomer and Dimer with TIMP-1 and TIMP-2*—Previously, we reported the binding affinities of pro-MMP-9 and MMP-9 with TIMP-1 and TIMP-2 using SPR (30). Here we used SPR to examine the binding kinetics of purified pro-MMP-9$_M$ and pro-MMP-9$_D$ and their active species with TIMP-1 and TIMP-2. As expected, pro-MMP-9$_M$ and pro-MMP-9$_D$ did not bind to TIMP-2. However, the active MMP-9 species demonstrated distinct association and dissociation phases of binding to TIMP-2. The calculated association rate constant ($k_a$), dissociation rate constant ($k_d$), and equilibrium constant ($K_d$) values from the SPR analyses are summarized in Table II. These analyses indicated the exist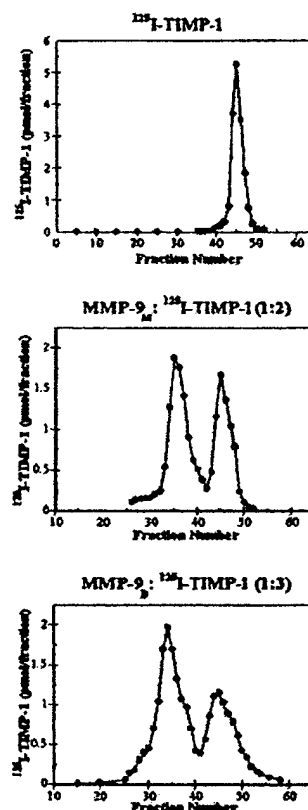ence of high and low affinity binding sites, as reported previously for the binding of TIMP-1 to pro-MMP-9 and MMP-9 (30), known to be a mixture of both monomeric and dimeric forms. The data also indicated a somewhat greater affinity (1.4–1.7-fold) of the dimeric form (latent and active) for TIMP-1 at the high affinity site (Table II). Both MMP-9$_M$ and MMP-9$_D$ bound to TIMP-2 with biphasic binding kinetics. However, the affinity of TIMP-2, at the high affinity site, for the active MMP-9 forms was ~2-fold lower than that exhibited by TIMP-1 (Table II).

*$K_i$ Determination of TIMP-1 and TIMP-2 for MMP-9$_M$ and MMP-9$_D$*—To further examine the binding of TIMP-1 and TIMP-2 to the purified MMP-9 forms, we carried out enzyme inhibition studies. As we have previously reported with MMP-2 and MMP-9 (30), TIMP-1 and TIMP-2 inhibited the active monomeric and dimeric species in a process consistent with slow binding inhibition (data not shown). Table III shows the $k_{on}$, $k_{off}$, and calculated $K_i$ values determined as described under "Experimental Procedures." TIMP-1 inhibits MMP-9$_M$ and MMP-9$_D$ with comparable rate constants for the inhibition onset ($k_{on}$) and recovery of activity ($k_{off}$), and therefore results in similar $K_i$ values. The $k_{on}$ is fast (>3 × 10$^5$ M$^{-1}$ s$^{-1}$) and $k_{off}$ is slow (~2.5 × 10$^{-3}$ s$^{-1}$), resulting in effective inhibition. The same trend is true for TIMP-2. The 3–5-fold difference between the $K_i$ values of TIMP-1 and TIMP-2 for the MMP-9 species is attributed to the $k_{on}$, which is 3–5-fold greater for TIMP-1 than for TIMP-2. The $k_{off}$ values of TIMP-1 and TIMP-2 for each MMP-9 species are essentially similar. The $k_{on}$ and $k_{off}$ values of TIMP-1 and TIMP-2 for MMP-9$_M$ and MMP-9$_D$ determined



FIG. 4. **Gel filtration of pro-MMP-9$_M$ and pro-MMP-9$_D$ with** $_{125}$**I-TIMP-1.** Purified pro-MMP-9$_M$ and pro-MMP-9$_D$ (10 pmol) were incubated (1 h, 22 °C) with 20 or 30 pmol of $^{125}$I-TIMP-1, respectively. The mixtures were then subjected to gel filtration using a Superose-12 column, as described under "Experimental Procedures." The radioactivity in the eluted fractions (350 μl) was measured in a γ counter, and the amount (picomoles) of TIMP-1 was determined from the specific activity.

---

[2] M. Pietila and R. Fridman, unpublished data.

*Monomeric and Dimeric Forms of Latent and Active MMP-9*

TABLE II

*Interactions of TIMPs with the latent and active monomeric and dimeric species of MMP-9, as evaluated by SPR*

TIMP-1 (69 pmol) and TIMP-2 (42 pmol) were immobilized onto activated CM5 sensor cells. The binding constants for each analyte protein were determined in duplicate using at least six different concentrations (2–400 nM) in a final volume of 200 $\mu$l of buffer W. The parameters $k_a$, $k_d$, and $K_d$ are defined under "Experimental Procedures."

| Analyte protein | $k_{a(1)}$[a] | $k_{a(2)}$ | $k_{d(1)}$ | $k_{d(2)}$ | $K_d$ | $K_d$ |
|---|---|---|---|---|---|---|
| | $M^{-1} s^{-1} \times 10^{-4}$ | $M^{-1} s^{-1} \times 10^{-4}$ | $s^{-1} \times 10^2$ | $s^{-1} \times 10^3$ | $\mu M$ | $nM$ |
| TIMP-1 | | | | | | |
| Pro-MMP-9$_M$ | 7.97 ± 0.47 | 1.01 ± 0.07 | 3.17 ± 0.09 | 3.65 ± 0.47 | 3.15 ± 0.51 | 45.8 ± 4.3 |
| Pro-MMP-9$_D$ | 14.3 ± 1.56 | 2.9 ± 0.29 | 4.66 ± 1.22 | 3.90 ± 1.13 | 2.26 ± 0.41 | 27.2 ± 5.4 |
| MMP-9$_M$ | 8.62 ± 0.65 | 0.93 ± 0.08 | 2.68 ± 0.53 | 3.67 ± 1.12 | 3.67 ± 0.31 | 42.5 ± 8.1 |
| MMP-9$_D$ | 14.5 ± 1.40 | 1.68 ± 0.21 | 4.29 ± 1.54 | 4.17 ± 1.35 | 2.56 ± 0.62 | 28.6 ± 7.4 |
| TIMP-2 | | | | | | |
| MMP-9$_M$ | 4.11 ± 0.33 | 1.36 ± 0.14 | 7.14 ± 1.73 | 4.02 ± 0.71 | 5.24 ± 0.90 | 98.0 ± 12.5 |
| MMP-9$_D$ | 8.80 ± 1.19 | 1.66 ± 0.31 | 8.93 ± 2.15 | 5.86 ± 2.25 | 5.37 ± 1.14 | 65.7 ± 17.1 |

[a] (1) and (2) refer to the first and the second phase of kinetics.

TABLE III

*Association, dissociation, and inhibition constants for MMP-9 monomer and dimer interactions with TIMPs*

To determine $k_{on}$ MMP-9$_M$ and MMP-9$_D$ were added to a 7 $\mu$M fluorogenic substrate solution in buffer R containing increasing TIMP-1 (0–30 nM) or TIMP-2 (0–60 nM) resulting in final enzyme concentrations of 1 and 0.5 nM, respectively. The dissociation rate constants were determined by diluting a preincubated (for 1 h at 25 °C) reaction mixture containing enzymes (300 nM) and inhibitors (330 nM) into 2 ml of a 12 $\mu$M fluorogenic substrate solution in buffer R, resulting in a final enzyme concentrations of 0.5 nM. All assays were carried out in triplicate. The $k_{on}$, $k_{off}$, and $K_i$ values were calculated as described under "Experimental Procedures."

| Enzyme | $k_{on}$ | $k_{off}$ | $K_i$ |
|---|---|---|---|
| | $M^{-1} s^{-1}$ | $s^{-1}$ | $nM$ |
| TIMP-1 | | | |
| MMP-9$_M$ | (3.12 ± 0.60) × 10⁵ | (2.55 ± 0.43) × 10⁻³ | 8.17 ± 1.11 |
| MMP-9$_D$ | (4.04 ± 0.28) × 10⁵ | (2.88 ± 0.11) × 10⁻³ | 7.13 ± 0.26 |
| TIMP-2 | | | |
| MMP-9$_M$ | (9.89 ± 0.98) × 10⁴ | (2.57 ± 0.23) × 10⁻³ | 25.9 ± 2.4 |
| MMP-9$_D$ | (8.44 ± 0.43) × 10⁴ | (3.05 ± 0.22) × 10⁻³ | 36.1 ± 2.2 |

from the inhibition experiments are in agreement with the values determined by SPR analyses (Table II). Hence, the calculated $K_i$ values of TIMP-1 and TIMP-2 were in the nanomolar range and within 2–5-fold of the $K_d$ values determined by SPR.

## DISCUSSION

Pro-MMP-9 is unique among the members of the MMP family in that it forms dimers consisting of covalently tethered monomers via a disulfide bond that can also be found in tissues. However, the biochemical properties of the monomeric and dimeric forms remained unknown. We have shown that the process of dimerization occurs intracellularly and concomitantly with glycosylation. Accordingly, both the precursor and mature forms of the pro-MMP-9$_D$ can be detected in the cellular compartment during pro-MMP-9 biosynthesis. However, only mature pro-MMP-9$_M$ and pro-MMP-9$_D$ are secreted. Under reducing conditions, only monomeric pro-MMP-9 was detected, consistent with disulfide-bond formation during intracellular dimerization. The identity of the cysteine residue(s) that predisposes pro-MMP-9 to dimerization is unknown. Based on the crystal structure of the homologue C-terminal domain of pro-MMP-2 (36), the conserved Cys[516] and Cys[704] in the hemopexin-like domain of pro-MMP-9 are likely to be disulfide-bonded precluding a role for these cysteine residues in dimer formation. Site directed mutagenesis studies also excluded Cys[674] in this process (27, 46). Consistently, a computational model of the three-dimensional structure of the hemopexin like-domain of pro-MMP-9,[3] based on the crystal structure of the same domain of pro-MMP-2 (39), suggests that Cys[674],

---

[3] I. Massova, L. Kotra, and S. Mobashery, unpublished data.

although unique to pro-MMP-9, is unlikely to be involved in dimerization, since it is solvent-inaccessible. Pro-MMP-9 contains an additional Cys at position 468 located in the collagen V-like hinge region that may be responsible for the dimerization. However, its role in dimer formation remains to be established.

Expression of pro-MMP-9 in the vaccinia system allowed us to obtain sufficient amount of recombinant enzyme for isolation and purification of the monomeric species from the dimeric form. Several procedures were tested to purify the monomer from the dimer including gelatin-affinity chromatography (27), ion-exchange chromatography, gel filtration, and glycerol gradient sedimentation. However, the latter proved to be the most efficient and consistent method to obtain homogeneous preparations of monomer and dimer. Purified pro-MMP-9$_M$ and pro-MMP-9$_D$ were examined for their interactions with TIMP-1 and TIMP-2 using gel filtration and SPR analyses. These studies showed that both pro-MMP-9 species could form stable complexes with TIMP-1 but not with TIMP-2. These data are in disagreement with a previous study showing a lack of complex formation between TIMP-1 and pro-MMP-9$_D$ (27). This discrepancy may be related to the method of purification of the monomeric from the dimeric form (gelatin-affinity chromatography (Ref. 27) *versus* glycerol-gradient sedimentation) and/or the use of recombinant TIMP-1 expressed in bacteria (27) *versus* mammalian cell-expressed TIMP-1 (this study). We have found that the binding of TIMP-1 to pro-MMP-9$_M$ or pro-MMP-9$_D$ was consistent with a stoichiometry of 1:1 and 2:1 molar ratio, respectively, suggesting that two high affinity binding sites for TIMP-1 are available in the dimeric form. These sites are likely to be located in the hemopexin-like domain, which is the major TIMP-1 binding site of pro-MMP-9 (44). The gel filtration data were supported by SPR analyses demonstrating binding of TIMP-1 to the monomer and dimer (latent and active) with biphasic kinetics. Thus, dimerization has no apparent effect on the binding kinetics of TIMP-1 and the affinity values are in agreement with our previous data with pro-MMP-9 and MMP-9, monomer and dimer mixtures (30). Although the nature of the second TIMP-1 binding site is unknown, the results presented here suggest that it is structurally different from the site required for dimerization since the dimer also binds TIMP-1. These results are in agreement with the study of Goldberg *et al.* (27) showing that mutations disrupting TIMP-1 binding had no effect on dimerization. Consistent with our previous SPR data with pro-MMP-9 (30) and the gel filtration experiments, TIMP-2 showed no binding to pro-MMP-9$_M$ or pro-MMP-9$_D$. However, both MMP-9$_M$ and MMP-9$_D$ exhibited biphasic TIMP-2 binding kinetics with an affinity that was ~2-fold lower than that exhibited by TIMP-1, at the high affinity site. Consistently, enzyme inhibition studies showed that both MMP-9$_M$ and MMP-9$_D$ were equally inhibited by

FIG. 5. **Stereo view of the energy-minimized computational model for the prodomain and the catalytic domain of pro-MMP-9.** The catalytic domain is shown in *green* with the active site depicted as a *green* surface. The catalytic zinc ion is depicted as an *orange sphere*. The backbone of the prodomain is represented as a *tube*. The backbone of the prodomain in *magenta* is released after the first hydrolytic step by stromelysin 1 at the Glu[59]-Met[60] peptide bond (indicated by the *arrow* at 7 o'clock). The remainder of the prodomain, given in *orange*, is released after the second hydrolytic step at the Arg[106]-Phe[107] peptide bond (indicated by the *arrow* at 9 o'clock). The side chains of residues Glu[59], Met[60], Arg[106], and Phe[107] are shown in the ball-and-stick representation. Cys[99], whose side chain thiol coordinates with the catalytic zinc ion, is shown in *yellow*.

TIMP-1 ($K_i$ = 7–8 nM) and TIMP-2 ($K_i$ = 26–36 nM) with kinetics consistent with slow binding inhibition, as previously reported (30). It should be noted that the $K_d$ values obtained by SPR analysis were concordant with the $K_i$ values obtained by enzyme inhibition studies.

Kinetic studies with MMP-9$_M$ and MMP-9$_D$ indicate no significant differences in the hydrolytic capacity of the MMP-9 forms against a fluorogenic peptide substrate and gelatin, a natural substrate of the enzyme (14). Furthermore, no evidence of cooperative interaction between the two active sites in terms of substrate hydrolysis and TIMP inhibition was observed, as determined by the enzyme kinetic studies with the peptide substrate. However, we have found a significant difference in the catalytic efficiency of pro-MMP-9$_M$ and pro-MMP-9$_D$ activation by stromelysin 1 with pro-MMP-9$_D$ being activated with a lower efficiency (10-fold), as indicated by $k_{cat}/K_m$ values for the activation reaction. The $K_m$ values are in the nanomolar range for both pro-MMP-9 forms, consistent with the fact that stromelysin 1 is readily saturated by pro-MMP-9 (44, 45). The $K_m$ values in the nanomolar range have also been observed for a number of proteolytic enzymes of the blood coagulation cascade with their substrates (47). Since catalysis is very slow, $K_m$ equals $K_s$. This indicates that the affinity ($K_s$) of stromelysin 1 for proMMP-9 is high. For the same reason, $k_{cat}$ = $k_2$. The microscopic rate constant $k_2$ is that for the peptide hydrolysis (hydrolytic) step, beyond the Michaelis-Menten complex. It is of interest that $k_{cat}$ values for turnover of the two forms of pro-MMP-9 are exceedingly small (in the range of $10^{-3}$ to $10^{-4}$ s$^{-1}$; Table I). A low $K_m$ is consistent with a low value for $k_{cat}$, since the ratio $k_{cat}/K_m$ has a limit set by the rate of diffusion. However, the resultant $k_{cat}/K_m$ values are in the respectable range of $10^4$ to $10^5$ M$^{-1}$ s$^{-1}$. These values further suggest that stromelysin 1 is an efficient physiological activator of pro-MMP-9 (48).

The low $k_{cat}$ values for activation of the two pro-MMP-9 forms by stromelysin 1 are worthy of comment. Highly catalyt-

ically competent enzymes, which often operate at the diffusion limit, may have $k_{cat}$ values in the range of $10^3$ s$^{-1}$. Clearly, stromelysin 1 does not merit this distinction. This raises the question: why is the $k_{cat}$ value for the activation of pro-MMP-9 so low? The crystal structure of the catalytic domain of stromelysin 1 indicates that the active site is an extended cleft (43, 49, 50). Proteases generally prefer unstructured peptides as substrates. This appears to be the case for stromelysin 1, based on the topology of its active site. The high affinity of stromelysin 1 for pro-MMP-9 indicates that the complex between the two enzymes forms readily, even in the nanomolar range for the pro-MMP-9 concentration. Despite this, turnover is slow ($t_{1/2}$ of 6.1 ± 0.3 and 28 ± 2 min computed from the $k_{cat}$ values for the monomeric and dimeric forms, respectively). Ogata *et al.* (45) first reported that the activation of pro-MMP-9 by stromelysin 1 is a sequential process involving two cleavage sites, first in the Glu[59]-Met[60] bond followed by the cleavage of the Arg[106]-Phe[107] peptide bond. The first cleavage generates an inactive 85-kDa intermediate form within seconds (44), whereas the second cleavage site generates the fully active 82-kDa MMP-9 species (29, 45). Fig. 5 shows a view of the energy-minimized computational model that we have generated for the catalytic domain of pro-MMP-9 and its requisite prodomain. As seen in this image, the Glu[59]-Met[60] bond is fully exposed near the surface of the protein, and hence would be accessible to stromelysin 1. Such a position would readily fit in the active site of stromelysin 1, and its hydrolysis is obviously rapid as discerned from the turnover in the range of several seconds. The fact that this cleavage occurs so readily facilitates measurement of the hydrolysis rate of the second cleavage, which results in zymogen activation. In essence, the product of the first cleavage, which is inactive, serves as the substrate for the activation event. Our model predicts that the Arg[106]-Phe[107] peptide bond is less accessible than the Glu[59]-Met[60] bond (Fig. 5). The kinetics of pro-MMP-9 activation by stromelysin 1, measured in

this study, are for the slow cleavage step and follow an uncomplicated standard profile for a single saturation event. For the second cleavage to take place, a required relaxation of structure will have to occur. This would entail dissociation of $Cys^{99}$ from coordination with the active site zinc ion (Fig. 5). It is necessary that after the formation of the pro-MMP-9/stromelysin 1 complex, pro-MMP-9 relaxes its secondary structure around the activation site, prior to its fitting into the active site of stromelysin 1 and hydrolysis of the peptide bond. This relaxation of structure should be the slow step in the catalytic turnover of pro-MMP-9.

The calculated $t_{1/2}$ for pro-MMP-9 turnover falls within the range of the length of time needed for larger scale motions of proteins, such as helix-coil transitions for example (51), which is consistent with our proposal for this local unfolding of the prodomain prior to its excision. It is also interesting to note that the pro-MMP-9$_D$ is substantially more stable than the monomer form, based on the $k_{cat}$ values that we have measured. This is explained intuitively by the observation that protein-protein interactions, in this case by dimerization, stabilize the protein making it more difficult to unfold. Thus, a possible, but yet unproven, explanation for the lower rate of dimer activation may be a reduced ability of the dimer to undergo the necessary relaxation of structure to permit the catalytic hydrolysis of the prodomain by stromelysin 1. The significance of the slower rate of activation of the pro-MMP-9 dimer by stromelysin 1 for MMP-9-dependent proteolysis is unclear. However, it is tempting to speculate that the existence of the slow activating dimer may provide an additional level of control during ECM degradation by MMP-9 species. Furthermore, fluctuations in the relative amounts of latent monomer and dimer secreted into the extracellular milieu may also play a role in the control of MMP-9-dependent proteolysis. The biochemical and cellular processes regulating dimerization of pro-MMP-9 remain to be determined.

REFERENCES

1. Wilhelm, S. M., Collier, I. E., Marmer, B. L., Eisen, A. Z., Grant, G. A., and Goldberg, G. I. (1989) *J. Biol. Chem.* **264**, 17213–17221
2. Vu, T. H., and Werb, Z. (1998) in *Gelatinase B: Structure, Regulation and Function; Matrix Metalloproteinases* (Parks, W. C., and Mecham, R. P., eds) pp. 115–148, Academic Press, San Diego
3. Ahrens, D., Koch, A. E., Pope, R. M., Stein-Picarella, M., and Niedbala, M. J. (1996) *Arthritis Rheum.* **39**, 1576–1587
4. Li, Y. Y., Feldman, A. M., Sun, Y., and McTiernan, C. F. (1998) *Circulation* **98**, 1728–34
5. Tamarina, N. A., McMillan, W. D., Shively, V. P., and Pearce, W. H. (1997) *Surgery* **122**, 264–272
6. Himelstein, B. P., Canete-Soler, R., Bernhard, E. J., Dilks, D. W., and Muschel, R. J. (1994) *Invasion Metastasis* **14**, 246–258
7. Sehgal, G., Hua, J., Bernhard, E. J., Sehgal, I., Thompson, T. C., and Muschel, R. J. (1998) *Am. J. Pathol.* **152**, 591–596
8. Ohno, I., Ohtani, H., Nitta, Y., Suzuki, J., Hoshi, H., Honma, M., Isoyama, S., Tanno, Y., Tamura, G., Yamauchi, K., Nagura, H., and Shirato, K. (1997) *Am. J. Respir. Cell. Mol. Biol.* **16**, 212–219
9. Agren, M. S., Jorgensen, L. N., Andersen, M., Viljanto, J., and Gottrup, F. (1998) *Br. J. Surg.* **85**, 68–71
10. Moses, M. A., Marikovsky, M., Harper, J. W., Vogt, P., Eriksson, E., Klagsbrun, M., and Langer, R. (1996) *J. Cell. Biochem.* **60**, 379–386
11. Canete-Soler, R., Gui, Y. H., Linask, K. K., and Muschel, R. J. (1995) *Dev. Dyn.* **204**, 30–40
12. Vu, T. H., Shipley, J. M., Bergers, G., Berger, J. E., Helms, J. A., Hanahan, D.,

13. Massova, I., Kotra, L. P., Fridman, R., and Mobashery, S. (1998) *FASEB J.* **12**, 1075–1095
14. Murphy, G., and Crabbe, T. (1995) *Methods Enzymol* **248**, 470–484
15. Gomez, D. E., Alonso, D. F., Yoshiji, H., and Thorgeirsson, U. P. (1997) *Eur. J. Cell Biol.* **74**, 111–122
16. Murphy, G., and Willenbrock, F. (1995) *Methods Enzymol.* **248**, 496–510
17. Goldberg, G. I., Marmer, B. L., Grant, G. A., Eisen, A. Z., Wilhelm, S., and He, C. S. (1989) *Proc. Natl. Acad. Sci. U. S. A.* **86**, 8207–8211
18. Bigg, H. F., Shi, Y. E., Liu, Y. E., Steffensen, B., and Overall, C. M. (1997) *J. Biol. Chem.* **272**, 15496–15500
19. Kjeldsen, L., Johnsen, A. H., Sengelov, H., and Borregaard, N. (1993) *J. Biol. Chem.* **268**, 10425–10432
20. Triebel, S., Blaser, J., Reinke, H., and Tschesche, H. (1992) *FEBS Lett.* **314**, 386–388
21. Toth, M., Gervasi, D. C., and Fridman, R. (1997) *Cancer Res.* **57**, 3159–3167
22. Moll, U. M., Youngleib, G. L., Rosinski, K. B., and Quigley, J. P. (1990) *Cancer Res.* **50**, 6162–6170
23. Vartio, T., and Baumann, M. (1989) *FEBS Lett.* **255**, 285–289
24. Mautino, G., Oliver, N., Chanez, P., Bousquet, J., and Capony, F. (1997) *Am. J. Respir. Cell. Mol. Biol.* **17**, 583–591
25. Upadhya, A. G., Harvey, R. P., Howard, T. K., Lowell, J. A., Shenoy, S., and Strasberg, S. M. (1997) *Hepatology* **26**, 922–928
26. Gonzalez-Avila, G., Iturria, C., Vadillo-Ortega, F., Ovalle, C., and Montano, M. (1998) *Pathobiology* **66**, 196–204
27. Goldberg, G. I., Strongin, A., Collier, I. E., Genrich, L. T., and Marmer, B. L. (1992) *J. Biol. Chem.* **267**, 4583–4591
28. Fridman, R., Fuerst, T. R., Bird, R. E., Hoyhtya, M., Oelkuct, M., Kraus, S., Komarek, D., Liotta, L. A., Berman, M. L., and Stetler-Stevenson, W. G. (1992) *J. Biol. Chem.* **267**, 15398–15405
29. Fridman, R., Toth, M., Pena, D., and Mobashery, S. (1995) *Cancer Res.* **55**, 2548–2555
30. Olson, M. W., Gervasi, D. C., Mobashery, S., and Fridman, R. (1997) *J. Biol. Chem.* **272**, 29975–29983
31. Gill, S. C., and von Hippel, P. H. (1989) *Anal. Biochem.* **182**, 319–326
32. Laemmli, U. K. (1970) *Nature* **227**, 680–685
33. Brown, P. D., Levy, A. T., Margulies, I. M., Liotta, L. A., and Stetler-Stevenson, W. G. (1990) *Cancer Res.* **50**, 6184–6191
34. Knight, C. G., Willenbrock, F., and Murphy, G. (1992) *FEBS Lett.* **296**, 263–266
35. Nagase, H., Fields, C. G., and Fields, G. B. (1994) *J. Biol. Chem.* **269**, 20952–20957
36. Knight, C. G. (1995) *Methods Enzymol.* **248**, 18–34
37. Morrison, J. F., and Walsh, C. T. (1988) *Adv. Enzymol. Relat. Areas Mol. Biol.* **61**, 201–301
38. Glick, B. R., Brubacher, L. J., and Leggett, D. J. (1978) *Can. J. Biochem.* **56**, 1055–1057
39. Libson, A. M., Gittis, A. G., Collier, I. E., Marmer, B. L., Goldberg, G. I., and Lattman, E. E. (1995) *Nat. Struct. Biol.* **2**, 938–942
40. Gohlke, U., Gomis-Ruth, F. X., Crabbe, T., Murphy, G., Docherty, A. J., and Bode, W. (1996) *FEBS Lett.* **378**, 126–130
41. Gomis-Ruth, F. X., Gohlke, U., Betz, M., Knauper, V., Murphy, G., Lopez-Otin, C., and Bode, W. (1996) *J. Mol. Biol.* **264**, 556–566
42. Pickford, A. R., Potts, J. R., Bright, J. R., Phan, I., and Campbell, I. D. (1997) *Structure* **5**, 359–370
43. Becker, J. W., Marcy, A. I., Rokosz, L. L., Axel, M. G., Burbaum, J. J., Fitzgerald, P. M., Cameron, P. M., Esser, C. K., Hagmann, W. K., Hermes, J. D., and Springer, J. P. (1995) *Protein Sci.* **4**, 1966–1976
44. O'Connell, J. P., Willenbrock, F., Docherty, A. J., Eaton, D., and Murphy, G. (1994) *J. Biol. Chem.* **269**, 14967–14973
45. Ogata, Y., Enghild, J. J., and Nagase, H. (1992) *J. Biol. Chem.* **267**, 3581–3584
46. Strongin, A. Y., Collier, I. E., Krasnov, P. A., Genrich, L. T., Marmer, B. L., and Goldberg, G. I. (1993) *Kidney Int.* **43**, 158–162
47. Mann, K. G., Nesheim, M. E., Church, W. R., Haley, P., and Krishnaswamy, S. (1990) *Blood* **76**, 1–16
48. Ramos-DeSimone, N., Hahn-Dantona, E., Sipley, J., Nagase, H., French, D. L., and Quigley, J. P. (1999) *J. Biol. Chem.* **274**, 13066–13076
49. Esser, C. K., Bugianesi, R. L., Caldwell, C. G., Chapman, K. T., Durette, P. L., Girotra, N. N., Kopka, I. E., Lanza, T. J., Levorse, D. A., MacCoss, M., Owens, K. A., Ponpipom, M. M., Simeone, J. P., Harrison, R. K., Niedzwiecki, L., Becker, J. W., Marcy, A. I., Axel, M. G., Christen, A. J., McDonnell, J., Moore, V. L., Olszewski, J. M., Saphos, C., Visco, D. M., Hagmann, W. K., et al. (1997) *J. Med. Chem.* **40**, 1026–1040
50. Finzel, B. C., Baldwin, E. T., Bryant, G. L., Jr., Hess, G. F., Wilks, J. W., Trepod, C. M., Mott, J. E., Marshall, V. P., Petzold, G. L., Poorman, R. A., O'Sullivan, T. J., Schostarez, H. J., and Mitchell, M. A. (1998) *Protein Sci.* **7**, 2118–2126
51. Brooks, C. L., Karplus, M., and Pettitt, B. M. (1988) *A Theoretical Perspective of Dynamics, Structure, and Thermodynamics*, John Wiley & Sons, New York

Shapiro, S. D., Senior, R. M., and Werb, Z. (1998) *Cell* **93**, 411–422

# Binding of Active (57 kDa) Membrane Type 1-Matrix Metalloproteinase (MT1-MMP) to Tissue Inhibitor of Metalloproteinase (TIMP)-2 Regulates MT1-MMP Processing and Pro-MMP-2 Activation*

Sonia Hernandez-Barrantes‡, Marta Toth‡, M. Margarida Bernardo, Maria Yurkova,
David C. Gervasi, Yuval Raz, QingXiang Amy Sang§, and Rafael Fridman¶

From the Department of Pathology and Karmanos Cancer Institute, Wayne State University, Detroit, Michigan 48201 and
the §Department of Chemistry, Biochemistry Division, Florida State University, Tallahassee, Florida 32306-4390

Previous studies have shown that membrane type 1-matrix metalloproteinase (MT1-MMP) (MMP-14) initiates pro-MMP-2 activation in a process that is tightly regulated by the level of tissue inhibitor of metalloproteinase (TIMP)-2. However, given the difficulty in modulating TIMP-2 levels, the direct effect of TIMP-2 on MT1-MMP processing and on pro-MMP-2 activation in a cellular system could not be established. Here, recombinant vaccinia viruses encoding full-length MT1-MMP or TIMP-2 were used to express MT1-MMP alone or in combination with various levels of TIMP-2 in mammalian cells. We show that TIMP-2 regulates the amount of active MT1-MMP (57 kDa) on the cell surface whereas in the absence of TIMP-2 MT1-MMP undergoes autocatalysis to a 44-kDa form, which displays a N terminus starting at $Gly^{285}$ and hence lacks the entire catalytic domain. Neither pro-MT1-MMP (N terminus $Ser^{24}$) nor the 44-kDa form bound TIMP-2. In contrast, active MT1-MMP (N terminus $Tyr^{112}$) formed a complex with TIMP-2 suggesting that regulation of MT1-MMP processing is mediated by a complex of TIMP-2 with the active enzyme. Consistently, TIMP-2 enhanced the activation of pro-MMP-2 by MT1-MMP. Thus, under controlled conditions, TIMP-2 may act as a positive regulator of MT1-MMP activity by promoting the availability of active MT1-MMP on the cell surface and consequently, may support pericellular proteolysis.

Turnover of extracellular matrix (ECM)[1] is a fundamental process of many normal and pathological conditions. A major group of enzymes responsible for ECM degradation is the matrix metalloproteinases (MMPs). The MMPs are multidomain

‡ Contributed equally to the results of this work.

¶ To whom all correspondence should be addressed: Dept. of Pathology, Wayne State University, 540 E. Canfield Ave., Detroit, MI 48201. Tel.: 313-577-1218; Fax: 313-577-8180; E-mail: rfridman@med.wayne.edu.

[1] The abbreviations used are: ECM, extracellular matrix; MMP, matrix metalloproteinase; TIMP, tissue inhibitor of metalloproteinase; PAGE, polyacrylamide gel electrophoresis; PBS, phosphate-buffered saline; mAb, monoclonal antibody; pAb, polyclonal antibody; pfu, plaque-forming units; FBS, fetal bovine serum; ECL, enhanced chemiluminescence; PM, plasma membrane; MT, membrane-type.

zinc-dependent endopeptidases that, with few exceptions, share a basic structural organization comprising a propeptide, catalytic, hinge, and C-terminal (hemopexin-like) domains (1, 2). All MMPs are produced in a latent form (pro-MMP) requiring activation for catalytic activity, a process that is usually accomplished by proteolytic removal of the propeptide domain. Once activated, all MMPs are specifically inhibited by a group of tissue inhibitors of metalloproteinases (TIMPs) (3).

Over the last five years, the MMP family has been expanded to include a new subfamily of membrane-tethered MMPs known as membrane-type MMPs (MT-MMPs), which as of today includes five enzymes: MT1-, MT2-, MT3-, MT4-, and MT5-MMP (4–8). The MT-MMPs, with the exception of MT4-MMP (9), are unique because they are anchored to the plasma membrane (PM) by means of a hydrophobic stretch of approximately 20 amino acids leaving the catalytic domain exposed to the extracellular space. MT1-MMP (MMP-14) was the first member of the MT-MMP family to be discovered and was identified as the first physiological activator of pro-MMP-2 (gelatinase A) (4, 10). The role of MT1-MMP in pericellular proteolysis is not restricted to pro-MMP-2 activation as MT1-MMP is a functional enzyme that can also degrade a number of ECM components (11–14) and hence can play a direct role in ECM turnover. MT1-MMP has been recently shown to be the first member of the MMP family indispensable for normal growth and development since mice deficient in MT1-MMP exhibit a variety of connective tissue pathologies and a short life span (15). MT1-MMP has also been shown to be a key enzyme in tumor metastasis and angiogenesis (16, 17).

Perhaps the most interesting aspect of MT1-MMP is the nature of its interactions with TIMP-2 and the role they play in pro-MMP-2 activation. Studies using PM extracts containing MT1-MMP (10) or a transmembrane-deleted form of MT1-MMP (18) have shown that, at low concentrations, TIMP-2 stimulates pro-MMP-2 activation whereas at high concentrations it inhibits activation. In addition, cross-linking experiments using PM preparations demonstrated the binding of TIMP-2 to MT1-MMP and to the hemopexin-like domain of pro-MMP-2 (10). Based on these observations, a model for the activation of pro-MMP-2 has been proposed in which the catalytic domain of MT1-MMP binds to the N-terminal portion of TIMP-2, leaving the negatively charged C-terminal region of TIMP-2 available for the binding of the hemopexin-like domain of pro-MMP-2 (10, 19). This ternary complex has been suggested to cluster pro-MMP-2 at the cell surface near a TIMP-2-free active MT1-MMP molecule, which is thought to initiate activation of the bound pro-MMP-2. Pro-MMP-2 activation would occur only at low TIMP-2 concentrations relative to

MT1-MMP, which would permit availability of active MT1-MMP to activate the pro-MMP-2 bound in the ternary complex. Thus, under restricted conditions, TIMP-2 is thought to promote the activation process by acting as a molecular link between MT1-MMP and pro-MMP-2. Kinetic studies with PM containing MT1-MMP (19) and studies with the catalytic domain of MT1-MMP immobilized on agarose beads (18) have supported this model. However, this model of pro-MMP-2 activation has not been established in a living cell system due to the difficulty in modulating the level of TIMP-2 expression.

Conflicting results have been reported regarding the MT1-MMP form(s) responsible for the formation of the MT1-MMP-TIMP-2 complex (10, 19–22). In fact, only a few studies examined the direct binding of TIMP-2 to full-length MT1-MMP. Strongin *et al.* (10) reported the binding of MT1-MMP from phorbol ester-treated HT-1080 PM to TIMP-2 bound to an MMP-2-C-terminal domain-affinity column. The bound MT1-MMP turned out to be the active enzyme starting at Tyr$^{112}$. Using radiolabeled TIMP-2 and PM extracts derived from COS-1 cells transfected with the full-length MT1-MMP cDNA, Zucker *et al.* (20) showed the formation of a ~80-kDa cross-linking product. However, the nature of the cross-linked MT1-MMP form(s) was not determined. Other studies showed the cross-linking of radiolabeled TIMP-2 with a purified autoactivated recombinant MT1-MMP lacking the transmembrane domain (13). However, binding of TIMP-2 to pro-MT1-MMP has not been examined. Finally, a 56-kDa form of MT1-MMP lacking the prodomain, found in the culture media of breast cancer cells, co-purified with TIMP-2 (23). Although various sources of MT1-MMP were used, these results were consistent with the active form of MT1-MMP being responsible for the binding of TIMP-2. Nonetheless, conflicting results were recently reported by Cao *et al.* (22), who proposed that the prodomain of MT1-MMP is essential for the binding of TIMP-2 to MT1-MMP and that pro-MT1-MMP can activate pro-MMP-2.

A major limitation in the study of MT1-MMP-TIMP-2 interactions has been the source of MT1-MMP, which included truncated enzymes and enzymes expressed in bacteria (18, 24). Furthermore, PM extracts (10, 19) and mammalian cells transfected with the MT1-MMP cDNA (4, 22, 25) contain endogenous TIMPs and/or MMPs. Thus, the direct contribution of TIMP-2 to pro-MMP-2 activation and its effect on MT1-MMP processing could not be clearly assessed. Here, a vaccinia virus expression system in mammalian cells (26–28), which allowed control of the level of TIMP-2 expression in the cells, was used to investigate the effect of various TIMP-2 levels on MT1-MMP processing and pro-MMP-2 activation and to identify the nature of the major MT1-MMP species detected.

## EXPERIMENTAL PROCEDURES

*Buffers*—The following buffers were used: collagenase buffer (50 mM Tris-HCl, pH 7.5, 5 mM CaCl$_2$, 150 mM NaCl, and 0.02% Brij-35), lysis buffer (25 mM Tris-HCl, pH 7.5, 1% IGEPAL CA-630: a non-ionic detergent from Sigma, 100 mM NaCl, 10 $\mu$g/ml aprotinin, 1 $\mu$g/ml leupeptin, 2 mM benzamidine, and 1 mM phenylmethylsulfonyl fluoride), HNTG buffer (50 mM Tris, pH 7.5, 150 mM NaCl, 0.1% IGEPAL, and 10% glycerol), harvest buffer (60 mM Tris-HCl, pH 7.5, 0.55% SDS, and 2 mM EDTA), and buffer R (50 mM HEPES, pH 7.5, 150 mM NaCl, 5 mM CaCl$_2$, 0.01% Brij-35, and 1% (v/v) dimethyl sulfoxide).

*Recombinant Vaccinia Viruses and Cell Culture*—The production of the recombinant vaccinia virus (vTF7-3) expressing bacteriophage T7 RNA polymerase has been described by Fuerst *et al.* (28). Recombinant vaccinia viruses, expressing either human TIMP-2 (vSC59-T2) or TIMP-1 (vT7-T1) were obtained by homologous recombination, as described previously (28, 29). To construct the recombinant vaccinia virus expressing human MT1-MMP, the full-length MT1-MMP cDNA (a generous gift from Dr. G. Goldberg, Washington University, St. Louis, MO) was amplified by polymerase chain reaction and then cloned into the pTF7EMCV-1 expression vector, under control of the T7 promoter (30). After sequence verification of the insert in both directions, the resulting

pTF7EMCV-1-MT1 plasmid was used to generate a recombinant vaccinia virus containing the full-length human MT1-MMP cDNA (vT7-MT1) by homologous recombination with wild type vaccinia virus, as described previously (26, 28). Non-malignant monkey kidney epithelial BS-C-1 (CCL-26) and human fibrosarcoma HT-1080 (CCL-121) cells were obtained from the American Type Culture Collection (ATCC, Rockville, MD) and cultured in Dulbecco's modified Eagle's medium supplemented with 10% fetal bovine serum (FBS) and antibiotics. HeLa S3 cells were obtained from ATCC (CCL-2.2) and grown in suspension in minimal essential Spinner medium (Quality Biologicals, Inc., Gaithersburg, MD) supplemented with 5% horse serum. All other tissue culture reagents were purchased from Life Technologies, Inc. (Grand Island, NY).

*Recombinant Proteins and Antibodies*—Human pro-MMP-2, TIMP-2, and TIMP-1 were expressed in HeLa S3 cells infected with the appropriate recombinant vaccinia viruses and purified to homogeneity, as described previously (26, 27, 31). The anti-TIMP-2 mAb CA101 (32) and a rabbit pAb to MT1-MMP (here referred to as pAb 437) (33) have been previously described. The rabbit pAb 160 and pAb 36 to MT1-MMP were generated and characterized, as described previously (34).

*Infection-Transfection and Pulse-Chase Analysis of MT1-MMP*—BS-C-1 cells in 6-well plates were infected with 30 plaque forming units (pfu)/cell of vTF7-3 for 45 min in Dulbecco's modified Eagle's medium containing 2.5% FBS. The media were then removed and the infected cells were transfected with 2 $\mu$g/ml of the pTF7EMCV-1-MT1 plasmid in Opti-MEM (Life Technologies, Inc.) (1 ml/well) using LipofectAMINE (Life Technologies, Inc.), as described by the manufacturer. After an incubation of 3.5 h, the medium was aspirated and replaced with 1 ml/well of Dulbecco's modified Eagle's medium without methionine supplemented with L-glutamine, 25 mM HEPES, pH 7.5, 0.1% dialyzed FBS, and 500 $\mu$Ci/ml [$^{35}$S]methionine (NEN Life Science Products Inc., Wilmington, DE). After a 15-min pulse, the plates were placed on ice, the medium was aspirated and the cells received 1 ml/well of chase media (Opti-MEM with 0.1% dialyzed FBS, 25 mM HEPES, pH 7.5, and 4.8 mM methionine). At the end of the chase period (0–120 min at 37 °C), the medium was aspirated and the cells were lysed with 100 $\mu$l/well of harvest buffer. The lysates were then subjected to five cycles of boiling and freezing followed by a brief centrifugation. The supernatants were collected into clean tubes with the addition of 5 mM iodoacetamide, 2.5% Triton X-100, and 20 $\mu$g/ml aprotinin (final concentrations). For immunoprecipitations, lysates were incubated (16 h, 4 °C) with 5 $\mu$g of the pAb 437 to MT1-MMP followed by addition of 30 $\mu$l of protein G-Sepharose beads for an additional overnight incubation at 4 °C. After recovering the beads by brief centrifugation, the supernatants were discarded and the beads were washed five times with cold HTNG buffer. The immunoprecipitates were recovered from the beads with 4× Laemmli sample buffer (35), boiled, and resolved by SDS-PAGE under reducing conditions followed by autoradiography.

*Expression of MT1-MMP and TIMP-2 by Infection*—To express MT1-MMP, BS-C-1 cells (10$^6$ cells/35-mm well) in 6-well plates were co-infected with 5 pfu/cell each of vTF7-3 and vT7-MT1 for 45 min in 0.5 ml/well of Dulbecco's modified Eagle's medium containing 2.5% FBS (infection medium) at 37 °C. In some experiments, the pfu/cell of the vT7-MT1 virus was varied (0–10 pfu/cell) to modulate the level of MT1-MMP expression. To co-express MT1-MMP with TIMP-2, and to modulate the level of inhibitor expression, BS-C-1 cells were co-infected with 5 pfu/cell each of vTF7-3 and vT7-MT1 and increasing amounts (0–10 pfu/cell) of vSC59-T2 for 45 min in 0.5 ml/well of infection medium at 37 °C. To co-express MT1-MMP and TIMP-1, the vSC59-T2 virus was replaced with vT7-T1. As a control, BS-C-1 cells were infected with the vTF7-3 virus alone at 5 pfu/cell. After the infection, the virus containing-medium was aspirated and each well received 2-ml of fresh infection medium without viruses. The infected cells were then incubated for a minimum of 6 h at 37 °C, before any further experimentation.

*Activation of Pro-MMP-2*—At the indicated times following infection, the medium was aspirated and replaced with 1 ml/well of Opti-MEM media (Life Technologies, Inc.) containing 2 nM recombinant pro-MMP-2. The cells were then incubated for various times at 37 °C. The medium was collected and clarified by a brief centrifugation (2,000 × g, 5 min) and the cells were solubilized in 100 $\mu$l/well of cold lysis buffer and centrifuged (13,000 × g) for 15 min at 4 °C. Samples of the medium (5 $\mu$l) and lysates (5 $\mu$l) were mixed with 4× Laemmli sample buffer (35) without reducing agents and without heating and subjected to gelatin zymography, as described previously (36).

*Immunoblot Analysis*—Infected BS-C-1 cells in 6-well plates, as described above, were lysed in cold lysis buffer (100 $\mu$l/well). The lysates (20 $\mu$l from each sample) were mixed with 4× Laemmli sample buffer

with β-mercaptoethanol and then resolved by reducing SDS-PAGE followed by immunoblot analysis using the appropriate antibodies. The immune complexes were detected using the ECL system (Pierce, Rockford, IL), according to the manufacturer's instructions.

*Surface Biotinylation*—Twenty-four hours post-infection, BS-C-1 cells in 150-mm tissue culture dishes were surface-biotinylated with 0.5 mg/ml of the water-soluble, cell impermeable, biotin analog sulfo-NHS-biotin (Pierce) for 30 min at 4 °C in PBS containing 0.1 mM $CaCl_2$ and 1 mM $MgCl_2$ (PBS-CM). The biotinylation reaction was quenched (10 min at 4 °C) with a freshly prepared solution of 50 mM $NH_4Cl$ in PBS-CM. After two washes with cold PBS-CM, the biotinylated cells were solubilized in harvest buffer (2 ml/150-mm dish), as described above. The lysates were then boiled (5 min), centrifuged (13,000 × $g$, 5 min) and the supernatants were supplemented with 2.5% Triton X-100 (final concentration). The lysates (500 μl) were immunoprecipitated with the appropriate antibody and protein G-Sepharose beads. The immunoprecipitates were resolved by reducing SDS-PAGE followed by blotting to a nitrocellulose membrane. The biotinylated proteins were detected with streptavidin-horseradish peroxidase and ECL.

*Isolation of PM*—BS-C-1 cells were infected with vaccinia viruses to express MT1-MMP alone or MT1-MMP with TIMP-2, as described above. The next day, the medium was aspirated and the cells were scraped into cold 25 mM Tris-HCl, 50 mM NaCl, pH 7.4. The samples were centrifuged (800 × $g$, 5 min) twice at 4 °C. The pellets were resuspended in the same buffer containing 8.5% sucrose, 10 μg/ml aprotinin, 2 μg/ml leupeptin, 1 mM phenylmethylsulfonyl fluoride, 4 mM benzamidine, and 10 mM N-ethylmaleimide. After sonication, the solutions were centrifuged at 19,000 × $g$ at 4 °C for 30 min. The supernatants were collected and centrifuged at 100,000 × $g$ at 4 °C for 1.25 h. The pellets were resuspended in the same buffer containing protease inhibitors and no sucrose. The PM fractions of HT-1080 cells treated (12 h, 37 °C) with 100 nM phorbol ester were prepared as described previously (36, 37).

*Activation of Pro-MMP-2 by PM of BS-C-1 Cells Co-expressing MT1-MMP and TIMP-2*—Pro-MMP-2 (55 nM) was incubated at 37 °C with each PM fraction (0.15 μg/μl) in a total volume of 200 μl of collagenase buffer. At varying times, 20 μl of the reaction mixture were added to acrylic cuvettes containing 2 ml of a 7 μM solution of the fluorescence quenched substrate $MOCAcPLGLA_2pr(Dnp)$-AR-$NH_2$ (Peptides International, Louisville, KY) (38) in buffer R, at 25 °C (31). Substrate hydrolysis was monitored with a Photon Technology International spectrofluorometer interfaced to a Pentium computer, equipped with the RatioMaster™ and FeliX™ hardware and software, respectively. The cuvette compartment was maintained at 25 °C. Fluorescence measurements were carried out at excitation and emission wavelengths of 328 and 393 nm and excitation and emission band passes of 1 and 3 nm, respectively. Less than 10% hydrolysis of the fluorogenic peptide substrate was monitored, as described by Knight (39). At the PM concentrations used, hydrolysis of this substrate by MT1-MMP was insignificant when compared with the hydrolysis by MMP-2.

*Coupling of TIMP-2 to Affi-Gel 10 Matrix*—Purified recombinant TIMP-2 (200 μg) in PBS was allowed to bind to 200 μl of Affi-Gel 10 (Bio-Rad) for 1 h at 22 °C with rotation. To block any active esters, 20 μl of 1 M ethanolamine-HCl, pH 8, were added to the reaction mixture followed by a 1-h incubation at 22 °C. The matrix (Affi-Gel 10-TIMP-2) was allowed to settle and the supernatant was subjected to reducing 12% SDS-PAGE to determine the amount of uncoupled TIMP-2. The Affi-Gel 10-TIMP-2 matrix was washed four times with PBS and equilibrated in collagenase buffer. The immobilized TIMP-2 maintained its capability to bind pro-MMP-2, as determined by SDS-PAGE analysis of the bound enzyme.

*Binding of MT1-MMP to Immobilized TIMP-2*—BS-C-1 cells in 150-mm dishes were infected to express MT1-MMP alone as described above. The cells were solubilized in lysis buffer (2 ml/dish) and the lysates (500 μl) were incubated (12 h, 4 °C) with a 50-μl suspension of either Affi-Gel 10-TIMP-2 matrix or Affi-Gel 10 matrix. The samples were centrifuged (13,000 × $g$, 5 min) and the supernatant (unbound fraction) and the matrix (bound fraction) were collected. The matrix beads were washed (5 times) with HNTG buffer. The beads and the unbound fraction (20 μl) were mixed with 20 μl of 4× Laemmli sample buffer with β-mercaptoethanol. The samples were then resolved by 12% SDS-PAGE followed by immunoblot analysis with the pAb 437, as described above.

*Co-immunoprecipitation of MT1-MMP with TIMP-2*—A pulse-chase experiment of MT1-MMP biosynthesis was carried out as described above except that the BS-C-1 cells were lysed in lysis buffer after the chase. Aliquots (20 μl) of the $^{35}$S-lysates were then incubated with or without unlabeled TIMP-2 (150 nM) for 2 h at 4 °C followed by immu-

noprecipitation with anti-TIMP-2 mAb CA101 and protein G-Sepharose beads, as described above. In parallel, another aliquot (20 μl) of the lysates received 10× harvest buffer followed by immunoprecipitation with the pAb 437 to anti-MT1-MMP, as described above. The immunoprecipitates were resolved by reducing SDS-PAGE followed by autoradiography.

*Immunoaffinity Purification and N-terminal Sequencing of MT1-MMP Species*—ImmunoPure Immobilized Protein A beads (Pierce) (1 ml) were incubated (1 h, 22 °C) with 2 ml of the pAb 437 serum in binding buffer (0.01 M sodium phosphate, pH 7.5–8.0, containing 150 mM NaCl). The beads were washed with 0.2 M sodium borate, pH 9.0, followed by coupling of the antibodies with 20 mM dimethyl pimelimidate hydrochloride in the same buffer for 30 min at 22 °C. The beads were then centrifuged (5 min, 2000 × $g$) and the supernatant was aspirated. The beads were resuspended in a solution of 0.2 M ethanolamine, pH 8.0, followed by a 2-h incubation with gentle rocking at room temperature. The pAb 437/Protein A beads were washed with binding buffer. BS-C-1 cells in eight 150-mm dishes infected to co-express MT1-MMP and TIMP-2 were lysed in harvest buffer. The lysate was supplemented with 2.5% Triton X-100 (final concentration) and incubated (12 h, 4 °C) with the pAb 437/Protein A beads. After a brief centrifugation, the beads were collected and washed three times with harvest buffer supplemented with 2.5% Triton X-100. The bound proteins were eluted with sample buffer, boiled, and subjected to reducing 10% SDS-PAGE in 1.5-mm wide gel cassettes and transferred to a polyvinylidene difluoride membrane (Bio-Rad). The transferred proteins were stained with 0.1% Coomassie Blue Brilliant R-250 in 1% acetic acid, 40% methanol. An aliquot of the eluted proteins was also subjected to immunoblot analysis using the pAb 437. After identification, the corresponding bands were cut out from the polyvinylidene difluoride membrane and sent for microsequencing to ProSeq (Boxford, MA).

## RESULTS

*Biosynthesis of Recombinant MT1-MMP and Activation of Pro-MMP-2*—To examine the expression and biosynthesis of MT1-MMP, BS-C-1 cells were infected with the vTF7-3 vaccinia virus and then transiently transfected with the pTF7EMCV-1-MT1 plasmid. After the infection-transfection procedure, the processing of MT1-MMP was examined by pulse-chase analysis followed by immunoprecipitation with the pAb 437. As shown in Fig. 1A, MT1-MMP was synthesized as a ~60-kDa protein that was sequentially processed to a major 57-kDa form and to a heterogeneous species of 44–40 kDa. Cleavage to the 57-kDa form was clearly detected after a 30-min chase period. After 45 min, the 44–40-kDa forms were detected. After 90 min, a ~35-kDa product was also immunoprecipitated by the pAb 437. In vTF7-3-infected but non-transfected BS-C-1 cells (Fig. 1A, *NT*), endogenous MT1-MMP was not detected demonstrating the lack of expression of endogenous enzyme in BS-C-1-infected cells.

The pTF7EMCV-1-MT1 plasmid was used to construct a recombinant vaccinia virus expressing full-length human MT1-MMP (vT7-MT1) by homologous recombination, as described previously (26, 28). BS-C-1 cells were co-infected with vTF7-3 and increasing pfu/cell of vT7-MT1 and then examined for their ability to activate exogenous pro-MMP-2. Generation of active MMP-2 in the media and the lysates was monitored by gelatin zymography. As shown in Fig. 1B, co-infection of BS-C-1 cells with vTF7-3 and vT7-MT1 resulted in pro-MMP-2 processing to the ~64-kDa intermediate form and the 62-kDa active species (14) in both the media and cell lysates. In contrast, BS-C-1 cells infected with the vTF7-3 virus alone failed to initiate pro-MMP-2 activation despite a small amount of autocatalytically generated MMP-2 present in the pro-MMP-2 stock solution. A very weak ~57-kDa gelatinolytic band was also detected in the lysates of cells co-infected with the two viruses but not with vTF7-3 alone. The 57-kDa form is derived from MT1-MMP, as will be discussed below. In the absence of exogenous pro-MMP-2, infected BS-C-1 cells showed no detectable levels of endogenous pro-MMP-2 (data not shown), as previously reported (26, 27).
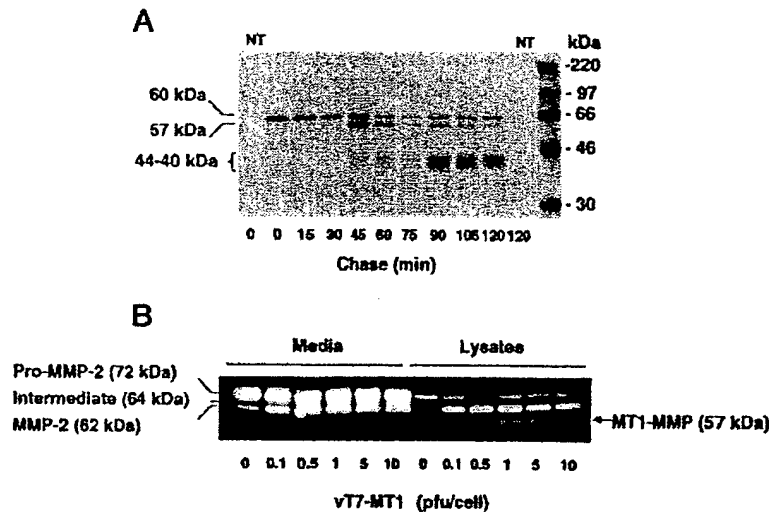
A



B



FIG. 1. **Processing and activity of MT1-MMP.** *A*, BS-C-1 cells were infected (45 min) with 30-pfu/cell of vTF7-3 and then transfected with 2 μg/well of the pTF7EMCV-1-MT1 expression vector. At 3.5 h post-infection transfection, the cells were pulse-labeled with [$^{35}$S]methionine for 15 min and then chased for 0–120 min. At the indicated times, the cells were lysed in harvest buffer and the lysates were immunoprecipitated with the pAb 437 and protein G-Sepharose beads. The immunoprecipitates were resolved by 10% SDS-PAGE under reducing conditions followed by autoradiography. *NT*, BS-C-1 cells infected with the vTF7-3 virus but not transfected and processed at 0 and 120 min. *B*, BS-C-1 cells were infected with 5 pfu/cell of vTF7-3 or co-infected with 5 pfu/cell of vTF7-3 and increasing pfu/cell (0.1–10) of vT7-MT1 to express MT1-MMP. At 12 h post-infection, the cells were incubated with 2 nM exogenous pro-MMP-2 for an additional 7 h at 37 °C. The medium (5 μl) and lysates (5 μl) were then harvested and analyzed by gelatin zymography.

*Effects of TIMP-2 on Pro-MMP-2 Activation and MT1-MMP Processing*—Previous *in vitro* studies demonstrated a role for TIMP-2 in pro-MMP-2 activation by MT1-MMP (10, 18, 19). However, the role of TIMP-2 in pro-MMP-2 activation has not been established in a cell-based assay. To investigate the role of TIMP-2 in MT1-MMP-dependent activation of pro-MMP-2, we used the vaccinia system to co-express MT1-MMP with TIMP-2 in BS-C-1 cells using the appropriate recombinant vaccinia viruses. To vary the level of inhibitor in the system, BS-C-1 cells were co-infected with various amounts (pfu/cell) of vSC59-T2, the TIMP-2-expressing vaccinia virus, while keeping constant the amount of vT7-MT1, thus varying the MT1-MMP/TIMP-2 ratio. It should be noted that all cells were infected with the polymerase-expressing virus (vTF7-3). After infection, the cells were incubated with exogenous pro-MMP-2. The lysates were then analyzed for MT1-MMP and TIMP-2 expression by immunoblot analysis (Fig. 2A) and pro-MMP-2 activation was monitored by gelatin zymography of the media and the lysates (Fig. 2B). As shown in the immunoblot of Fig. 2A, the level of TIMP-2 expression was dependent on the amounts (pfu/cell) of vSC59-T2 virus used to infect the cells. Under the same conditions, BS-C-1 cells infected to express MT1-MMP alone showed no detectable expression of endogenous TIMP-2 by immunoblot analysis (Fig. 2A) and by ELISA determination (data not shown), in agreement with our previous studies in vaccinia-infected cells (26, 27, 31).

Immunoblot analysis of the same lysates with the anti-MT1-MMP pAb 437 showed a profile of MT1-MMP forms that varied with the level of TIMP-2 expression. In the absence of TIMP-2, the lysates exhibited the 60- and 44–40-kDa species of MT1-MMP with the latter being the major species. Increased expression of TIMP-2 correlated with the accumulation of the 57-kDa species of MT1-MMP, which was concomitant with a gradual decrease in the 44–40-kDa forms. The 57-kDa species of MT1-MMP detected in the co-infected cells co-migrated with the MT1-MMP form present in the PM of phorbol ester-treated HT-1080 cells (Fig. 2A, lane c). Lack of a direct correlation between the intensity of the bands corresponding to the 44–40-kDa species and the intensity of the bands corresponding to the 60- and 57-kDa forms may be due to a differential solubi-

lization of these forms from the cells when using Nonidet P-40 (IGEPAL) as detergent. Indeed, extraction with SDS (harvest buffer) significantly improved the yield and detection of the 60-kDa species of MT1-MMP (data not shown).

Zymographic analysis (Fig. 2B) showed that the activation of pro-MMP-2 by MT1-MMP, as determined by the appearance of the 62-kDa species of MMP-2, was dependent on the level of TIMP-2 expression. Low levels of TIMP-2 expression correlated with an enhanced activation of pro-MMP-2 when compared with cells expressing MT1-MMP alone in both the media and the cell lysates. On the other hand, high levels of TIMP-2 expression were associated with lower amounts of active MMP-2 (62 kDa). In the lysates of cells co-expressing MT1-MMP and TIMP-2, we also detected a weak ~57-kDa-gelatinolytic band (Fig. 2B), which was identified as MT1-MMP (see Fig. 3). Time course analysis (Fig. 2C) of the activation process by MT1-MMP co-expressed with TIMP-2, revealed the presence of active MMP-2 (62 kDa) in the lysates as early as 30 min after addition of pro-MMP-2. At the same time, the enzyme in the medium remained mostly in the latent form. With time, the 62-kDa species was also detected in the medium suggesting that after surface activation the 62-kDa form dissociates from the cell surface and it is released into the medium (Fig. 2C).

*TIMP-2 but Not TIMP-1 Induces the Accumulation of the 57-kDa Form of MT1-MMP*—As shown above (Fig. 2), co-expression of MT1-MMP and TIMP-2 induced the accumulation of the 57-kDa species of MT1-MMP, which exhibited gelatinolytic activity. To further investigate the effects of TIMP-2 on the accumulation of the 57-kDa species and to compare its effect with that of TIMP-1, BS-C-1 cells were infected to express MT1-MMP alone or MT1-MMP with increasing amounts of either TIMP-2 or TIMP-1. These experiments were carried out in the absence of exogenous pro-MMP-2. Generation of the 57-kDa species was monitored by gelatin zymography and immunoblot analysis. As shown in Fig. 3A, the intensity of the 57-kDa gelatinolytic species increased as a function of the amount (pfu/cell) of the vSC59-T2 virus (Fig. 3A, lanes 4–6). On the other hand, lysates of cells expressing MT1-MMP alone (Fig. 3A, lane 3) showed little or no detectable gelatinolytic bands. Co-expression of MT1-MMP with TIMP-1 had no effect
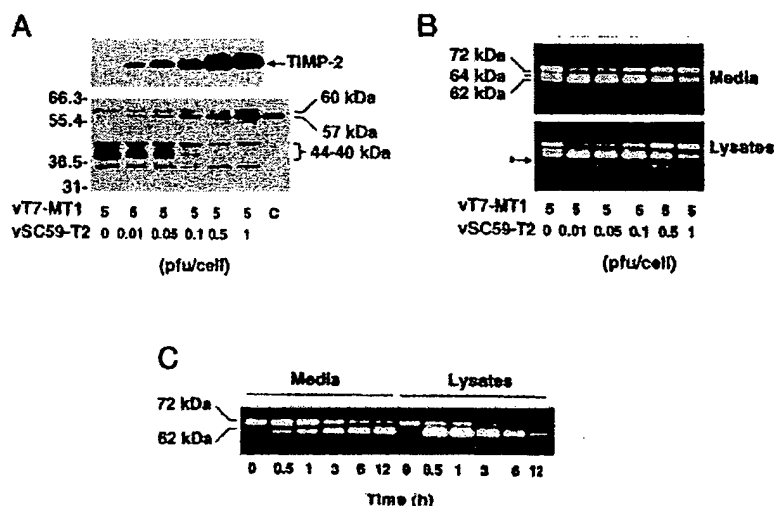
FIG. 2. TIMP-2 enhances the activation of pro-MMP-2 by MT1-MMP and induces the accumulation of the 57-kDa species of MT1-MMP. *A* and *B*, BS-C-1 cells were co-infected with 5 pfu/cell each of vTF7-3 and vT7-MT1 and increasing amounts of vSC59-T2 (0–1 pfu/cell) to co-express MT1-MMP and TIMP-2. At 6 h post-infection, the cells were incubated with 2 nM exogenous pro-MMP-2 for an additional 12 h at 37 °C followed by solubilization of the cell monolayer with lysis buffer. In *A*, lysates (20 μl) were subjected to reducing 12% SDS-PAGE followed by immunoblot analysis using the anti-TIMP-2 mAb (CA101) (*upper panel*) and the anti-MT1-MMP pAb 437 (*lower panel*). Detection of the antigens was performed using ECL (Pierce). As control (*lane C*), PM fractions (16 μg) of phorbol ester-treated HT-1080 cells were similarly analyzed. In *B*, the media and lysates (5 μl each) were subjected to gelatin zymography. *Asterisk* shows the 57-kDa MT1-MMP enzyme. *C*, BS-C-1 cells were co-infected with 5 pfu/cell each of vTF7-3 and vT7-MT1 and 0.01 pfu/cell of vSC59-T2. At 6 h post-infection, the cells were incubated with 2 nM exogenous pro-MMP-2 for various times (0–12 h). At each time, the medium and lysates were harvested and analyzed by gelatin zymography. These experiments were repeated at least three times with similar results.
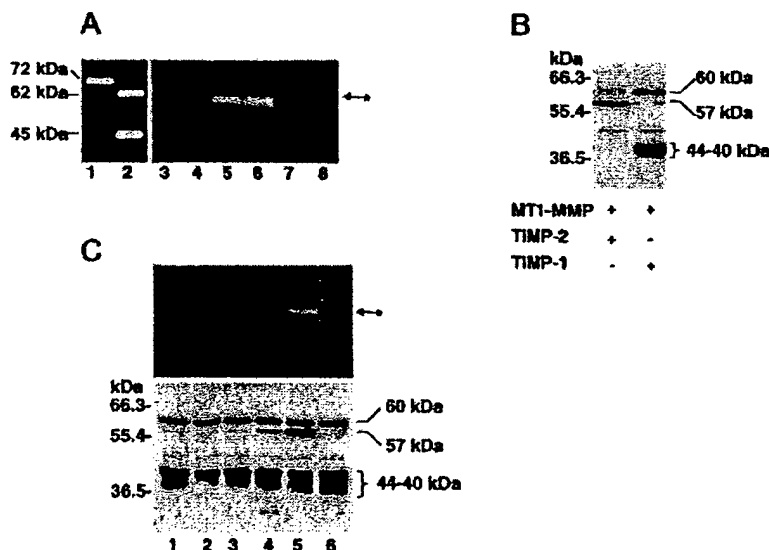


FIG. 3. Effect of TIMP-2 and TIMP-1 on the profile of MT1-MMP forms. *A*, BS-C-1 were co-infected with 5 pfu/cell each of vTF7-3 and vT7-MT1 (*lanes 3–8*) and increasing amounts of vSC59-T2 (*lane 4*, 0.01 pfu/cell; *lane 5*, 0.1 pfu/cell; *lane 6*, 1 pfu/cell) or vT7-T1 (*lane 7*, 0.01 pfu/cell; *lane 8*, 1 pfu/cell). At 12 h post-infection, the cells were harvested in 100 μl of lysis buffer and the lysates (20 μl) were analyzed by gelatin zymography. *Lane 1* shows purified pro-MMP-2 (5 ng) and *lane 2* shows active MMP-2 (62 and 45 kDa) (5 ng), as references. *B*, BS-C-1 cells were co-infected with 5 pfu/cell each of vTF7-3 and vT7-MT1 and either vSC59-T2 (5 pfu/cell) to co-express TIMP-2 or vT7-T1 (5 pfu/cell) to co-express TIMP-1. The lysates were resolved by reducing 12% SDS-PAGE followed by immunoblot analysis using the pAb 437 and detection by ECL. *C*, BS-C-1 cells were co-infected with 5 pfu/cell each of vTF7-3 and vT7-MT1. After infection, the cells were incubated (12 h, 37 °C) without (*lane 1*) or with increasing amounts of either exogenous TIMP-2 (*lane 2*, 1 ng/ml; *lane 3*, 10 ng/ml; *lane 4*, 100 ng/ml; *lane 5*, 500 ng/ml) or TIMP-1 (*lane 6*, 500 ng/ml). The lysates were harvested and analyzed by gelatin zymography and immunoblot analysis with the pAb 437 to MT1-MMP. *Asterisks* in *A* and *C* show the 57-kDa MT1-MMP gelatinolytic enzyme.

on the gelatinolytic activity (Fig. 3*A, lanes 7* and *8*) and on the profile of the MT1-MMP forms (Fig. 3*B*) when compared with cells co-expressing MT1-MMP and TIMP-2 (Fig. 3*B*) or MT1-MMP alone (shown in Fig. 3*C, lane 1*).

The accumulation of the 57-kDa species was also observed after addition of exogenous TIMP-2 to cells expressing MT1-MMP. As shown in Fig. 3*C*, 500 ng of TIMP-2 (Fig. 3*C, lane 5*) clearly induced the appearance of the 57-kDa gelatinolytic form

when compared with cells that did not receive the inhibitor (Fig. 3*C, lane 1*). Consistently, immunoblot analysis of the same lysates showed a dose-dependent accumulation of the 57-kDa species after addition of exogenous TIMP-2 (Fig. 3*C, lanes 4* and *5*). Under these conditions, reduction in the relative amounts of the 44–40-kDa species of MT1-MMP was not evident. This suggests that exogenous TIMP-2, as opposed to inhibitor co-expressed with MT1-MMP (Fig. 3*B*), is less effi-
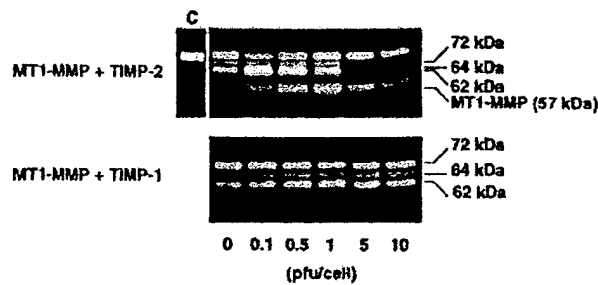
FIG. 4. **TIMP-2 but not TIMP-1 regulates the MT1-MMP-dependent activation of pro-MMP-2.** BS-C-1 cells were co-infected with 5 pfu/cell each of vTF7-3 and vT7-MT1 and increasing amounts (0–10 pfu/cell) of either vSC59-T2 (MT1-MMP + TIMP-2) or vT7-T1 (MT1-MMP + TIMP-1). At 6 h post-infection, the cells were incubated with 2 nM exogenous pro-MMP-2 for an additional 10 h at 37 °C. The lysates were then harvested and analyzed by gelatin zymography. *Lane c* shows pro-MMP-2 incubated with BS-C-1 cells infected with 5 pfu/cell of vTF7-3 alone. These experiments were repeated at least three times with similar results.

cient in preventing the generation of the 44–40-kDa forms. Addition of exogenous TIMP-1 (500 ng) had no effect on the appearance of the 57-kDa gelatinolytic species and did not alter the profile of MT1-MMP forms, as determined by zymography and immunoblot analysis, respectively (Fig. 3C, lane 6).

We then compared the effects of TIMP-2 and TIMP-1 on the ability of MT1-MMP to initiate pro-MMP-2 activation. To this end, BS-C-1 cells were infected to express MT1-MMP with either TIMP-2 or TIMP-1 using the appropriate vaccinia viruses as described under "Experimental Procedures." After infection, the cells were examined for their ability to initiate pro-MMP-2 activation by gelatin zymography. As shown in Fig. 4, TIMP-2 enhanced the MT1-MMP-dependent activation of pro-MMP-2 at low inhibitor concentrations when compared with MT1-MMP alone. At high inhibitor concentrations (5–10 pfu/cell of vSC59-T2), a significant inhibition of pro-MMP-2 activation was observed. In addition, the presence of TIMP-2 correlated with the appearance of the 57-kDa species of MT1-MMP. In contrast to TIMP-2, co-expression of MT1-MMP with TIMP-1 had little or no effect on the rate of pro-MMP-2 activation (Fig. 4) and the 57-kDa form was not detected in the lysates.

*Effect of TIMP-2 on the Cellular Distribution of MT1-MMP Forms*—We investigated the effect of TIMP-2 on the nature of the MT1-MMP forms expressed on PM isolated from co-infected BS-C-1 cells. As shown in Fig. 5A, the PM of BS-C-1 cells expressing only MT1-MMP contained the 60- and 44–40-kDa forms, as determined by immunoblot analysis using the pAb 437 (Fig. 5A, lane 3). Co-expression of MT1-MMP and TIMP-2 correlated with the detection of both the 60- and 57-kDa forms in the PM whereas the amount of the 44–40-kDa species was significantly reduced (Fig. 5A, lane 4). PM of control cells (infected with vTF7-3 alone) showed neither MT1-MMP forms (Fig. 5A, lane 2), as expected. PM of phorbol ester-treated HT-1080 cells were analyzed in parallel and found to contain the 57-kDa form of MT1-MMP, as a major enzyme species (Fig. 5A, lane 1). The PM fractions were also examined for the presence of TIMP-2 (Fig. 5B). As expected, TIMP-2 was only detected in the PM of BS-C-1 cells co-expressing MT1-MMP and TIMP-2 (Fig. 5B, lane 4) and in the PM of HT-1080 cells (Fig. 5B, lane 1).

The surface association of MT1-MMP and TIMP-2 in BS-C-1 cells expressing MT1-MMP with or without TIMP-2 was examined by surface biotinylation followed by immunoprecipitation with the appropriate antibodies. The 60- and 44–40-kDa forms of MT1-MMP were the major surface-biotinylated species immunoprecipitated from cells expressing MT1-MMP alone (Fig.

5C, lane 1), in agreement with the results obtained with the PM fractions. As expected, no biotinylated endogenous TIMP-2 was immunoprecipitated from the same sample (Fig. 5C, lane 3). In the cells co-infected to express MT1-MMP and TIMP-2, the 57-kDa form of MT1-MMP was also surface-biotinylated, in addition to the 60- and 44–40-kDa forms (Fig. 5C, lane 4). TIMP-2 was also detected on the cell surface (Fig. 5C, lane 6) suggesting its association with MT1-MMP. The specificity of these procedures was demonstrated by the lack of signal in the absence of antibodies (Fig. 5C, lanes 2 and 5). A similar profile of MT1-MMP forms was previously reported by Lehti et al. (25) on the surface of phorbol ester-treated HT-1080 cells, which are known to express TIMP-2 (10, 19). These results also demonstrate that the processing and cellular localization of MT1-MMP forms in the vaccinia-infected cells is similar to that found in cells naturally expressing MT1-MMP.

We next examined the ability of the PM fractions derived from cells expressing MT1-MMP alone (containing the 60- and 44–40-kDa species) or MT1-MMP with TIMP-2 (containing the 60- and 57-kDa species) (shown in Fig. 5A) to initiate pro-MMP-2 activation as described under "Experimental Procedures." As shown in Fig. 5D, the PM fraction of cells expressing MT1-MMP alone was unable to initiate pro-MMP-2 activation over a 5-h period, as determined by the background activity measured with a fluorescence quenched substrate (38). In contrast, pro-MMP-2 incubation with PM derived from cells co-expressing MT1-MMP and TIMP-2 resulted in a 12-fold enhancement of MMP-2 activity over that measured with PM of cells expressing MT1-MMP alone. It should be mentioned that the PM fraction capable of activating pro-MMP-2 was derived from cells infected to express MT1-MMP with relatively low amounts of TIMP-2 (0.1 pfu/cell of vSC59-T2) since high levels of TIMP-2 expression resulted in PM fractions unable to generate MMP-2 activity (data not shown). Taken together, these results suggest that the 57-kDa species of MT1-MMP is required for pro-MMP-2 activation.

*The 57-kDa Species of MT1-MMP Binds TIMP-2*—Previous studies demonstrated that MT1-MMP could form a complex with TIMP-2 on the cell surface (10). Our studies indicated that three major forms of MT1-MMP (60-, 57-, and 44–40 kDa) were present on the surface of cells with the amount of the 57-kDa species increasing in the presence of TIMP-2. In addition, our studies with BS-C-1 cells co-infected to express MT1-MMP and TIMP-2 showed that these cells exhibited surface expression of TIMP-2 suggesting that the inhibitor was interacting with MT1-MMP. Therefore, we asked which of the MT1-MMP forms could bind TIMP-2. To this end, samples of various time points of a pulse-chase experiment were incubated with or without exogenous unlabeled TIMP-2 and then subjected to immunoprecipitation with anti-TIMP-2. As shown in Fig. 6A, the samples from the 0, 45-, and 90-min chase periods contained the 60-, 57-, and/or the 44–40-kDa forms of MT1-MMP, as demonstrated after immunoprecipitation with the pAb 437. Addition of unlabeled TIMP-2 and the anti-TIMP-2 mAb to each of these samples revealed that, under these conditions, only the ^{35}S-labeled 57-kDa form of MT1-MMP co-precipitated with the inhibitor (Fig. 6A). In the absence of TIMP-2, no signal was detected with the anti-TIMP-2 antibody (data not shown).

To further examine the nature of the MT1-MMP species capable of binding TIMP-2, we used an Affi-Gel 10-TIMP-2-affinity matrix. To this end, lysates were prepared from BS-C-1 cells expressing MT1-MMP alone since co-expression with TIMP-2 would have affected binding to the affinity matrix. As shown in Fig. 6B, the 57-kDa species bound to the TIMP-2-affinity matrix (Fig. 6B, lane 1) whereas the 60- and 44–40-
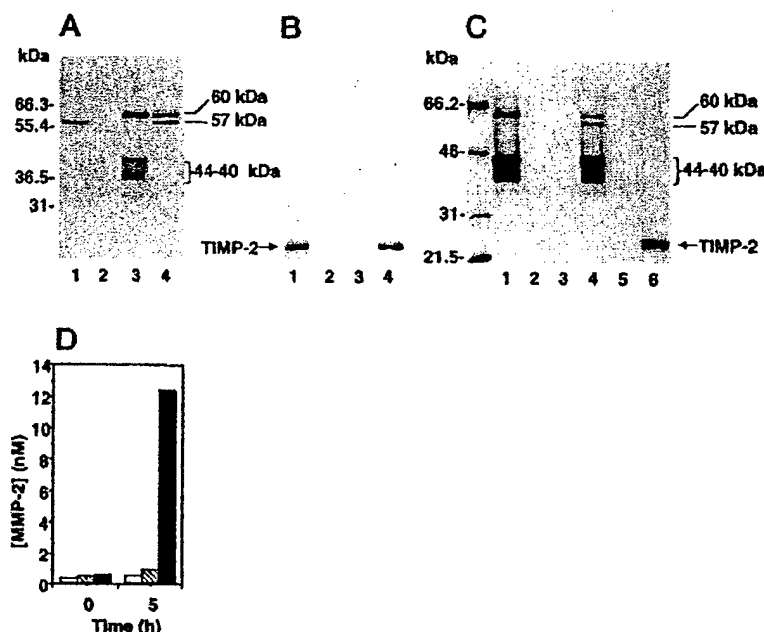
FIG. 5. **Effect of TIMP-2 on the PM localization and surface association of MT1-MMP forms.** *A* and *B*, immunoblot analysis of MT1-MMP and TIMP-2 in PM fractions. PM (12 μg/lane) isolated from BS-C-1 cells infected with 5 pfu/cell each of vTF7-3 and vT7-MT1 to express MT1-MMP (*lane 3*) or co-infected with vT7-MT1 (5 pfu/cell) and vSC59-T2 (0.1 pfu/cell) to co-express MT1-MMP and TIMP-2 (*lane 4*) were subjected to reducing 10% SDS-PAGE followed by immunoblot analysis with pAb 437 to MT1-MMP (*A*) or with a mAb to TIMP-2 (*B*). As controls, PM isolated from BS-C-1 cells infected with the vTF7-3 virus alone (*lane 2*) and of phorbol ester-treated HT-1080 cells (16 μg) (*lane 1*) were analyzed in parallel. *C*, biotinylation of MT1-MMP forms in BS-C-1 cells co-infected to express MT1-MMP alone (*lanes 1–3*) or MT1-MMP and TIMP-2 (*lanes 4–6*) as described above. The lysates (500 μl) were immunoprecipitated with either the pAb 437 to MT1-MMP (*lanes 1* and *4*) or the mAb CA101 to TIMP-2 (*lanes 3* and *6*) and protein G-Sepharose beads. As controls, the lysates received protein G-Sepharose beads without antibody (*lanes 2* and *5*). The immunoprecipitates were resolved by reducing 12% SDS-PAGE followed by blotting to a nitrocellulose membrane and detection by streptavidin-horseradish peroxidase and ECL. The biotinylated molecular weight markers shown are from Bio-Rad. *D*, activation of pro-MMP-2 by PM. Pro-MMP-2 (55 nM), in collagenase buffer, was incubated at 37 °C in the absence (*open bar*) and presence of PM (0.15 μg/μl) isolated from BS-C-1 cells infected to express MT1-MMP (*hatched bar*) or co-express MT1-MMP and TIMP-2 (*black bar*), as described above (*A*). MMP-2 activity was measured at 0 and 5 h incubation as described under "Experimental Procedures." Similar results were obtained in two independent experiments.

kDa forms of MT1-MMP did not (Fig. 6*B, lane 3*) in agreement with the co-immunoprecipitation experiment. These results also show that although cells expressing MT1-MMP alone contain low levels of the 57-kDa species of MT1-MMP, this form can be enriched by the affinity step. The 57-kDa species failed to bind to the TIMP-2 affinity column in the presence of 5 mM EDTA (data not shown). No binding of MT1-MMP species was detected to the affinity matrix without TIMP-2 (Fig. 6*B, lane 2*). PM fractions isolated from phorbol ester-treated HT-1080 cells containing only the 57-kDa species were used as positive control (Fig. 6*B, lane 4*).

*N Termini of the MT1-MMP Species*—To define the nature of the MT1-MMP species including the TIMP-2-binding 57-kDa form, a lysate of BS-C-1 cells infected to co-express MT1-MMP and TIMP-2 to induce accumulation of the 57-kDa species was subjected to immunoaffinity purification as described under "Experimental Procedures." The 60-, 57-, and 44-kDa (upper band) MT1-MMP species were isolated from the lysates and subjected to N-terminal sequencing. As shown in Fig. 7, the isolated 57-kDa form of MT1-MMP displays a N terminus starting at Tyr[112] and therefore is identical to the active species of MT1-MMP previously reported (10, 25). The N terminus of the 60-kDa species starts at Ser[24] demonstrating that this species is the latent form (pro-MT1-MMP) (1). The 44-kDa form starts at Gly[285], which is at the beginning of the hinge region (1, 8), and therefore lacks the complete catalytic domain. In agreement with the N-terminal sequencing data, a pAb to the propeptide domain of pro-MT1-MMP (pAb 36) (34) failed to recognize both the 57- and 44-kDa species (data not shown).

## DISCUSSION

A cellular approach designed to express MT1-MMP in the absence or presence of TIMP-2 facilitated the characterization of the three major MT1-MMP species and revealed a unique interaction between MT1-MMP and TIMP-2 by which the inhibitor regulates the nature of MT1-MMP enzymes on the cell surface. The results presented here demonstrate that the concentration of active MT1-MMP (57 kDa) on the cell surface was directly and positively regulated by TIMP-2. Absence of inhibitor, on the other hand, resulted in a significant decrease in the amount of active enzyme on the cell surface leading to the generation of a membrane-bound inactive 44-kDa species, which was further processed to lower molecular weight forms. N-terminal sequencing of the 44-kDa species revealed that this form starts at Gly[285] and hence lacks the entire catalytic domain but maintains the hemopexin-like domain and the hinge region (1). A previous study reported a N-terminal sequence of a 43-kDa species of MT1-MMP starting at Ile[256] in the catalytic domain (25). This species was isolated from the media of HT-1080 cells transfected to overexpress a soluble transmembrane-deleted MT1-MMP and therefore the enzyme and/or mechanism responsible for MT1-MMP cleavage in solution could not be established. Although both the previously reported 43-kDa form (25) and the 44-kDa species identified in the present study are functionally inactive, our sequencing data were obtained with wild type MT1-MMP and therefore the N terminus of the 44-kDa species is likely to represent a true cleavage site.

Previous studies implicated MMP-2 in the processing of active MT1-MMP to the 44-kDa species (40, 41). However, our results clearly show that this process is MMP-2 independent
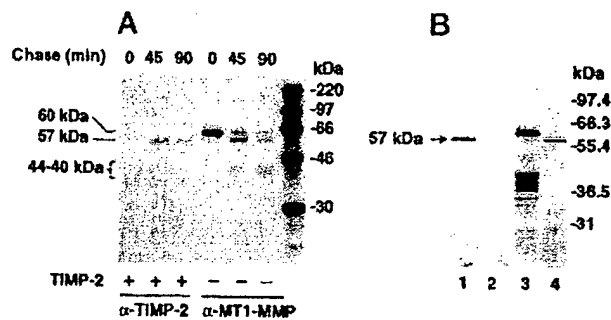
FIG. 6. **The 57-kDa form of MT1-MMP binds TIMP-2.** *A,* BS-C-1 cells were infected-transfected to express MT1-MMP as described in the legend to Fig. 1A. Three and half hours post-infection, the cells were pulse-labeled with [$^{35}$S]methionine for 15 min and chased for 90 min. At various times (0, 45, and 90 min), the cells were harvested in lysis buffer. A fraction of the lysates (20 μl) was incubated (2 h, 4 °C) with 150 nM unlabeled TIMP-2 (+) and then immunoprecipitated with the mAb to TIMP-2 (α-TIMP-2). In parallel, another fraction of the lysates (20 μl), which did not receive unlabeled TIMP-2 (−), was supplemented with harvest buffer to immunoprecipitate MT1-MMP with the pAb 437 (α-MT1-MMP), as described under "Experimental Procedures." The immunoprecipitates were resolved on 10% SDS-PAGE under reducing conditions followed by autoradiography. *B,* BS-C-1 cells were infected to express MT1-MMP. The next day, the cells were lysed in lysis buffer. The lysates (500 μl each) were incubated (12 h, 4 °C) with either Affi-Gel 10-TIMP-2 matrix (*lanes 1* and *3*) or Affi-Gel 10 matrix without immobilized TIMP-2 (*lane 2*) (50 μl suspension each). The bound fraction was eluted with 20 μl of Laemmli sample buffer with β-mercaptoethanol. The samples (bound and unbound) were resolved by 12% SDS-PAGE followed by immunoblot analysis with the pAb 437 to MT1-MMP. *Lane 1,* fraction bound to Affi-Gel 10-TIMP-2 matrix; *lane 2,* fraction bound to Affi-Gel 10 matrix; *lane 3,* unbound fraction from Affi-Gel 10-TIMP-2 matrix; and *lane 4,* PM of phorbol ester-treated HT-1080 cells, as control.

since vaccinia-infected BS-C-1 cells do not produce detectable pro-MMP-2 (26, 27). Cleavage at the Gly-Gly$^{285}$ peptide bond and consequent generation of the 44-kDa species was significantly inhibited by TIMP-2, as shown in cells co-expressing MT1-MMP and TIMP-2. Ellebroeck *et al.* (40) reported a reduction of the 44-kDa species in concanavalin A-treated ovarian carcinoma cells receiving exogenous TIMP-2. However, the effects of TIMP-2 on the profile of the MT1-MMP forms could not be differentiated from the pleiotrophic effects of concanavalin A, which may include effects on TIMP-2 and/or MT1-MMP expression as well as effects on cellular organization and plasma membrane structure. A recent study indicated that TIMP-2 modulates MT1-MMP activity in melanoma cells. However, a direct correlation between TIMP-2 expression and MT1-MMP processing could not be established (42). Based on the results in the vaccinia system, which allowed modulation of the level of TIMP-2 expression in the cells, we can conclude that the accumulation of the 57-kDa species of MT1-MMP and the reduction in the amount of the 44-kDa forms is a sole consequence of the presence of TIMP-2. The fact that TIMP-2, but not TIMP-1, inhibited the generation of the 44-kDa species further demonstrates that MT1-MMP processing is an autocatalytic event. The lack of effect of TIMP-1 is consistent with the weak inhibitory activity of TIMP-1 for MT1-MMP, as previously reported (12, 43). However, the inhibitory effect of TIMP-2 can be mimicked by general synthetic MMP inhibitors (40, 41) or by exposure of cells to concanavalin A or phorbol ester, which may induce TIMP-2 expression.

Due to the difficulty in modulating the level of MT1-MMP and TIMP-2 expression in cells the direct contribution of TIMP-2 to the activation of pro-MMP-2 could not be established in a cell-based system. The data presented here show for the first time in a living cellular system that pro-MMP-2 activation by wild type MT1-MMP is tightly regulated by the level of
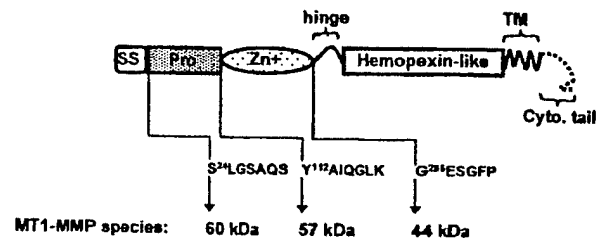


FIG. 7. **N-terminal sequence of MT1-MMP forms.** Diagram of the location and sequence of the MT1-MMP forms isolated. *SS,* signal sequence; *pro,* propeptide domain; *Zn$^+$,* catalytic domain; *TM,* transmembrane region; *Cyto. tail,* cytoplasmic tail.

TIMP-2 expression in the cells. These results are consistent with the biphasic role of TIMP-2 in pro-MMP-2 activation as first proposed by Strongin *et al.* (10) *in vitro.* The stimulatory effect of TIMP-2 on pro-MMP-2 activation has been attributed to the formation of a ternary complex between MT1-MMP, TIMP-2, and pro-MMP-2 (10, 18, 19). However, our data show that BS-C-1 cells expressing MT1-MMP alone were able to initiate pro-MMP-2 activation suggesting that TIMP-2, and hence ternary complex formation, may not be an absolute requirement for pro-MMP-2 activation. Consistently, a C-terminal truncated TIMP-2, unable to form a complex with pro-MMP-2, and marimastat, a synthetic MMP inhibitor, can promote, at relatively low concentrations, the accumulation of active MT1-MMP and consequently the activation of pro-MMP-2.[2] Under these conditions, the surface association of pro-MMP-2 is likely to be mediated by other factors, which may include stable structural elements and/or nonspecific adsorption. Previous studies have shown that the association of pro-MMP-2 with the cell surface can be mediated by a variety of factors including ECM components (44, 45), heparin (19), and/or the integrin α,β$_3$ (46).

Our findings suggest that the effects of TIMP-2 on pro-MMP-2 activation may also be related to its ability to control the amount of active MT1-MMP in the cells by preventing the autocatalytic processing of active MT1-MMP on the cell surface. This is based on the observation that co-expression of MT1-MMP with increasing levels of TIMP-2 produced a gradual accumulation of the 57-kDa species that correlated, at the lowest level of inhibitor, with enhanced pro-MMP-2 activation when compared with cells expressing MT1-MMP alone. Thus, by binding and inhibiting a fraction of active MT1-MMP, TIMP-2 reduces the extent of autocatalytic processing of free 57-kDa species and therefore promotes its accumulation on the cell surface, which in turn enhances pro-MMP-2 activation. However, the ratio between free and TIMP-2-bound (inhibited) active (57 kDa) MT1-MMP has yet to be determined. At high inhibitor concentrations, activation of pro-MMP-2 was significantly diminished despite the higher amounts of 57-kDa MT1-MMP detected under those conditions. A plausible explanation for this apparent inconsistency may be the titration of all active MT1-MMP species by TIMP-2, which results in inhibition of pro-MMP-2 activation as previously proposed (18, 19). Furthermore, the maximum pro-MMP-2 activation observed at the lowest level of the 57-kDa species detected in the cells may reflect the high catalytic efficiency of active and TIMP-2-free MT1-MMP toward pro-MMP-2. This may also be the case in cells infected to express only MT1-MMP. Our data suggest that the 57-kDa species of MT1-MMP is the major pro-MMP-2 activator. This species is the active enzyme form, as determined by N-terminal sequencing, and its appearance correlated with
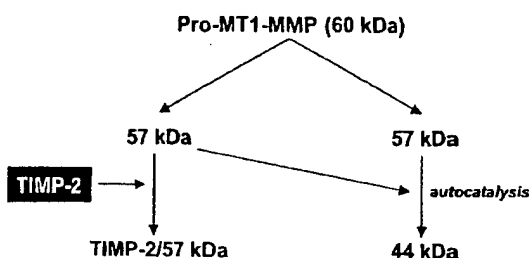
**Pro-MT1-MMP (60 kDa)**



FIG. 8. Diagram of MT1-MMP processing and interactions with TIMP-2.

enhanced pro-MMP-2 activation. In addition, we have shown that only PM fractions containing the 57-kDa species (derived from cells co-expressing MT1-MMP and TIMP-2) were able to initiate pro-MMP-2 activation whereas PM fractions lacking the 57-kDa species had no activity toward pro-MMP-2. Finally, the 57-kDa species co-migrated with the 57-kDa species of MT1-MMP detected in PM fractions of phorbol ester-treated HT-1080 cells, which were shown to activate pro-MMP-2 (10, 37, 47) and to contain mostly active MT1-MMP (10, 19).

The nature of the MT1-MMP species responsible for TIMP-2 binding remains controversial. Both latent (21, 22) and active species (10) of MT1-MMP have been implicated in binding to the inhibitor. The data presented here are consistent with the 57-kDa species of MT1-MMP being the major TIMP-2 binding form. Co-immunoprecipitation and TIMP-2 affinity experiments demonstrated that the 57-kDa species of MT1-MMP bound to TIMP-2, whereas pro-MT1-MMP and the 44-kDa form showed no binding under the same conditions suggesting that the latter forms exhibit a reduced affinity for TIMP-2. Considering that the 57-kDa species starts at $Tyr^{112}$ and that pro-MT1-MMP showed no significant TIMP-2 binding, it is reasonable to assume that TIMP-2 interacts with the active site of MT1-MMP (48). Furthermore, the binding of TIMP-2 to the 57-kDa species was abolished in the presence of EDTA, suggesting that the catalytic $Zn^{2+}$ ion is required for TIMP-2 binding. These results are not consistent with the propeptide domain of pro-MT1-MMP being required for TIMP-2 binding (22).

Fig. 8 depicts a model of MT1-MMP processing and its regulation by TIMP-2. Cells produce pro-MT1-MMP that is activated by a pro-convertase-dependent mechanism (14, 49). Activation may occur in the trans-Golgi network and/or at the cell surface, as furin is also targeted to the PM and to the extracellular space (50, 51). Surface-anchored active MT1-MMP (57 kDa) is a fully functional enzyme capable of pericellular proteolysis. However, in the absence of TIMP-2, the 57-kDa species undergoes autocatalytic conversion to a 44-kDa inactive membrane-tethered form by cleavage at the hinge region ($Gly^{285}$), which diminishes the surface availability of active MT1-MMP. The 44-kDa form is further processed to a series of lower molecular weight degradation products. Under these conditions, the extent of MT1-MMP-dependent proteolysis would be determined by a balance between pro-MT1-MMP expression and activation, the rate of autocatalytic processing and enzyme internalization. Binding of TIMP-2 to activated MT1-MMP (57 kDa) inhibits autocatalysis and consequently, active enzyme accumulates on the cell surface as cells produce more MT1-MMP. This suggests that, under conditions of low levels of TIMP-2 expression relative to MT1-MMP, TIMP-2 may act as a positive regulator of MT1-MMP activity and therefore may enhance pericellular proteolysis including pro-MMP-2 activation and ECM degradation. The 57-kDa·TIMP-2 complex also favors the localization of pro-MMP-2 (by ternary complex formation) on the cell surface thereby promoting pro-MMP-2 ac-

tivation (10, 19). However, other pro-MMP-2-cell surface interaction could play a role (19, 44, 46). Excess TIMP-2, relative to MT1-MMP, will eventually block all active MT1-MMP inhibiting proteolysis. This model reflects the dynamic and unique interactions between MT1-MMP and TIMP-2 in living cells that tightly regulate MT1-MMP pericellular activity.

## REFERENCES

1. Massova, I., Kotra, L. P., Fridman, R., and Mobashery, S. (1998) *FASEB J.* **12,** 1075–1095
2. Birkedal-Hansen, H., Moore, W. G., Bodden, M. K., Windsor, L. J., Birkedal-Hansen, B., DeCarlo, A., and Engler, J. A. (1993) *Crit. Rev. Oral Biol. Med.* **4,** 197–250
3. Murphy, G., and Willenbrock, F. (1995) *Methods Enzymol.* **248,** 496–510
4. Sato, H., Takino, T., Okada, Y., Cao, J., Shinagawa, A., Yamamoto, E., and Seiki, M. (1994) *Nature* **370,** 61–65
5. Takino, T., Sato, H., Shinagawa, A., and Seiki, M. (1995) *J. Biol. Chem.* **270,** 23013–23020
6. Will, H., and Hinzmann, B. (1995) *Eur. J. Biochem.* **231,** 602–608
7. Puente, X. S., Pendas, A. M., Llano, E., Velasco, G., and Lopez-Otin, C. (1996) *Cancer Res.* **56,** 944–949
8. Pei, D. (1999) *J. Biol. Chem.* **274,** 8925–8932
9. Itoh, Y., Kajita, M., Kinoh, H., Mori, H., Okada, A., and Seiki, M. (1999) *J. Biol. Chem.* **274,** 34260–34266
10. Strongin, A. Y., Collier, I., Bannikov, G., Marmer, B. L., Grant, G. A., and Goldberg, G. I. (1995) *J. Biol. Chem.* **270,** 5331–5338
11. d'Ortho, M. P., Will, H., Atkinson, S., Butler, G., Messent, A., Gavrilovic, J., Smith, B., Timpl, R., Zardi, L., and Murphy, G. (1997) *Eur. J. Biochem.* **250,** 751–757
12. d'Ortho, M. P., Stanton, H., Butler, M., Atkinson, S. J., Murphy, G., and Hembry, R. M. (1998) *FEBS Lett.* **421,** 159–164
13. Ohuchi, E., Imai, K., Fujii, Y., Sato, H., Seiki, M., and Okada, Y. (1997) *J. Biol. Chem.* **272,** 2446–2451
14. Pei, D., and Weiss, S. J. (1996) *J. Biol. Chem.* **271,** 9135–9140
15. Holmbeck, K., Bianco, P., Caterina, J., Yamada, S., Kromer, M., Kuznetsov, S. A., Mankani, M., Robey, P. G., Poole, A. R., Pidoux, I., Ward, J. M., and Birkedal-Hansen, H. (1999) *Cell* **99,** 81–92
16. Hiraoka, N., Allen, E., Apel, I. J., Gyetko, M. R., and Weiss, S. J. (1998) *Cell* **95,** 365–377
17. Sato, H., Okada, Y., and Seiki, M. (1997) *Thromb. Haemostasis* **78,** 497–500
18. Kinoshita, T., Sato, H., Okada, A., Ohuchi, E., Imai, K., Okada, Y., and Seiki, M. (1998) *J. Biol. Chem.* **273,** 16098–16103
19. Butler, G. S., Butler, M. J., Atkinson, S. J., Will, H., Tamura, T., van Westrum, S. S., Crabbe, T., Clements, J., d'Ortho, M. P., and Murphy, G. (1998) *J. Biol. Chem.* **273,** 871–880
20. Zucker, S., Drews, M., Conner, C., Foda, H. D., DeClerck, Y. A., Langley, K. E., Bahou, W. F., Docherty, A. J., and Cao, J. (1998) *J. Biol. Chem.* **273,** 1216–1222
21. Cao, J., Rehemtulla, A., Bahou, W., and Zucker, S. (1996) *J. Biol. Chem.* **271,** 30174–30180
22. Cao, J., Drews, M., Lee, H. M., Conner, C., Bahou, W. F., and Zucker, S. (1998) *J. Biol. Chem.* **273,** 34745–34752
23. Imai, K., Ohuchi, E., Aoki, T., Nomura, H., Fujii, Y., Sato, H., Seiki, M., and Okada, Y. (1996) *Cancer Res.* **56,** 2707–2710
24. Lichte, A., Kolkenbrock, H., and Tschesche, H. (1996) *FEBS Lett.* **397,** 277–282
25. Lehti, K., Lohi, J., Valtanen, H., and Keski-Oja, J. (1998) *Biochem. J.* **334,** 345–353
26. Fridman, R., Fuerst, T. R., Bird, R. E., Hoyhtya, M., Oelkuct, M., Kraus, S., Komarek, D., Liotta, L. A., Berman, M. L., and Stetler-Stevenson, W. G. (1992) *J. Biol. Chem.* **267,** 15398–15405
27. Fridman, R., Bird, R. E., Hoyhtya, M., Oelkuct, M., Komarek, D., Liang, C. M., Berman, M. L., Liotta, L. A., Stetler-Stevenson, W. G., and Fuerst, T. R. (1993) *Biochem. J.* **289,** 411–6
28. Fuerst, T. R., Earl, P. L., and Moss, B. (1987) *Mol. Cell. Biol.* **7,** 2538–2544
29. Moss, B. (1992) *Bio/Technology* **20,** 345–362
30. Elroy-Stein, O., Fuerst, T. R., and Moss, B. (1989) *Proc. Natl. Acad. Sci. U. S. A.* **86,** 6126–6130
31. Olson, M. W., Gervasi, D. C., Mobashery, S., and Fridman, R. (1997) *J. Biol. Chem.* **272,** 29975–29983
32. Hoyhtya, M., Fridman, R., Komarek, D., Porter-Jordan, K., Stetler-Stevenson, W. G., Liotta, L. A., and Liang, C. M. (1994) *Int. J. Cancer* **56,** 500–505
33. Gervasi, D. C., Raz, A., Dehem, M., Yang, M., Kurkinen, M., and Fridman, R. (1996) *Biochem. Biophys. Res. Commun.* **228,** 530–538
34. Li, H., Bauzon, D. E., Xu, X., Tschesche, H., Cao, J., and Sang, Q. A. (1998) *Mol. Carcinog.* **22,** 84–94
35. Laemmli, U. K. (1970) *Nature* **227,** 680–685
36. Toth, M., Gervasi, D. C., and Fridman, R. (1997) *Cancer Res.* **57,** 3159–3167
37. Strongin, A. Y., Marmer, B. L., Grant, G. A., and Goldberg, G. I. (1993) *J. Biol. Chem.* **268,** 14033–14039
38. Knight, C. G., Willenbrock, F., and Murphy, G. (1992) *FEBS Lett.* **296,** 263–266
39. Knight, C. G. (1995) *Methods Enzymol.* **248,** 18–34
40. Ellerbroek, S. M., Fishman, D. A., Kearns, A. S., Bafetti, L. M., and Stack, M. S. (1999) *Cancer Res.* **59,** 1635–1641
41. Stanton, H., Gavrilovic, J., Atkinson, S. J., d'Ortho, M. P., Yamada, K. M., Zardi, L., and Murphy, G. (1998) *J. Cell Sci.* **111,** 2789–2798
42. Kurschat, P., Zigrino, P., Nischt, R., Breitkopf, K., Steurer, P., Klein, C. E., Krieg, T., and Mauch, C. (1999) *J. Biol. Chem.* **274,** 21056–21062
43. Will, H., Atkinson, S. J., Butler, G. S., Smith, B., and Murphy, G. (1996) *J. Biol. Chem.* **271,** 17119–17123
44. Steffensen, B., Bigg, H. F., and Overall, C. M. (1998) *J. Biol. Chem.* **273,**

20622–20628
45. Wallon, U. M., and Overall, C. M. (1997) *J. Biol. Chem.* **272,** 7473–7481
46. Brooks, P. C., Stromblad, S., Sanders, L. C., von Schalscha, T. L., Aimes, R. T., Stetler-Stevenson, W. G., Quigley, J. P., and Cheresh, D. A. (1996) *Cell* **85,** 683–693
47. Fridman, R., Toth, M., Pena, D., and Mobashery, S. (1995) *Cancer Res.* **55,** 2548–2555

48. Fernandez-Catalan, C., Bode, W., Huber, R., Turk, D., Calvete, J. J., Lichte, A., Tschesche, H., and Maskos, K. (1998) *EMBO J.* **17,** 5238–5248
49. Sato, H., Kinoshita, T., Takino, T., Nakayama, K., and Seiki, M. (1996) *FEBS Lett.* **393,** 101–104
50. Mallet, W. G., and Maxfield, F. R. (1999) *J. Cell Biol.* **146,** 345–359
51. Vey, M., Schafer, W., Berghofer, S., Klenk, H. D., and Garten, W. (1994) *J. Cell Biol.* **127,** 1829–1842